Brigham Young University
BYU ScholarsArchive

All Theses and Dissertations

2018-04-01

# Nonlinear Model Predictive Control for a Managed Pressure Drilling with High-Fidelity Drilling Simulators

Junho Park
*Brigham Young University*

Follow this and additional works at: https://scholarsarchive.byu.edu/etd

Part of the Chemical Engineering Commons

BYU ScholarsArchive Citation

Park, Junho, "Nonlinear Model Predictive Control for a Managed Pressure Drilling with High-Fidelity Drilling Simulators" (2018). *All Theses and Dissertations*. 6792.
https://scholarsarchive.byu.edu/etd/6792

This Thesis is brought to you for free and open access by BYU ScholarsArchive. It has been accepted for inclusion in All Theses and Dissertations by an authorized administrator of BYU ScholarsArchive. For more information, please contact scholarsarchive@byu.edu, ellen_amatangelo@byu.edu.

المنارة للاستشارات

www.manaraa.com

# Nonlinear Model Predictive Control for a Managed Pressure Drilling with

# High-Fidelity Drilling Simulators

Junho Park

A thesis submitted to the faculty of
Brigham Young University
in partial fulfillment of the requirements for the degree of

Master of Science

John D. Hedengren, Chair
S. Andrew Ning
Matthew J. Memmott

Department of Chemical Engineering

Brigham Young University

Copyright © 2018 Junho Park

All Rights Reserved

المنارة للاستشارات

www.manaraa.com

# ABSTRACT

## Nonlinear Model Predictive Control for a Managed Pressure Drilling with High-Fidelity Drilling Simulators

Junho Park
Department of Chemical Engineering, BYU
Master of Science

The world's energy demand has been rapidly increasing and is projected to continue growing for at least the next two decades. With increasing global energy demand and competition from renewable energy, the oil and gas industry is striving for more efficient petroleum production. Many technical breakthroughs have enabled the drilling industry to expand the exploration to more difficult drilling such as deepwater drilling and multilateral directional drilling. For example, managed pressure drilling (MPD) offers ceaseless operation with multiple manipulated variables (MV) and wired drill pipe (WDP) provides two-way, high-speed measurements from bottom hole and along-string sensors. These technologies have maximum benefit when applied in an automation system or as a real-time advisory tool. The objective of this study is to investigate the benefit of nonlinear model-based control and estimation algorithms with various types of models. This work presents a new simplified flow model (SFM) for bottomhole pressure (BHP) regulation in MPD operations. The SFM is embedded into model-based control and estimation algorithms that use model predictive control (MPC) and moving horizon estimation (MHE), respectively. This work also presents a new Hammerstein-Wiener nonlinear model predictive controller for BHP regulation. Hammerstein-Wiener models employ input and output static nonlinear blocks before and after linear dynamics blocks to simplify the controller design. The control performance of the new Hammerstein-Wiener nonlinear controller is superior to conventional PID controllers in a variety of drilling scenarios. Conventional controllers show severe limitations in MPD because of the interconnected multivariable and nonlinear nature of drilling operations. BHP control performance is evaluated in scenarios such as drilling, pipe connection, kick attenuation, and mud density displacement and the efficacy of the SFM and Hammerstein-Wiener models is tested in various control schemes applicable to both WDP and mud pulse systems. Trusted high-fidelity drilling simulators are used to simulate well conditions and are used to evaluate the performance of the controllers using the SFM and Hammerstein-Wiener models. The comparison between non-WDP (semi-closed loop) and WDP (full-closed loop) applications validates the accuracy of the SFM under the set of conditions tested and confirms comparability with model-based control and estimation algorithms. The SFM MPC maintains the BHP within ± 1 bar of the setpoint for each investigated scenario, including for pipe connection and mud density displacement procedures that experience a wider operation range than normal drilling.

Keywords: managed pressure drilling, nonlinear model predictive control, moving horizon estimation, Hammerstein-Wiener MPC, simplified drilling flow model

المنارة للاستشارات
www.manaraa.com

# ACKNOWLEDGMENTS

I would first like to thank my advisor, Dr. John Hedengren, for his constant support and guidance. His positive energy always gave me confidence, encouragement, and renewed motivation. In my experience he has not only been a good mentor, but a good friend to me and each of his other students. He has always listened carefully to me and has never limited my ideas or potential. Without his consistent thoughtfulness and patience, the path I've taken for the past several years would have been much more rugged and challenging.

I would also like to express my appreciation to Cameron Price and Thomas Webber, both of whom provided significant assistance to me in my research. Their eagerness to learn lent synergy to my research and inspired me in my determination to push my work forward. I also thank all of the PRISM students who did not hesitate to share valuable results and findings from their research: Ammon Eaton, Reza Asgharzadeh, Mostafa Safdarnegad, Logan Beal, Abe Martin, Trent Okeson, Nathaniel Gates, Brigham Hansen, Sam Thorpe, Damon Peterson, and Cody Simmons.

I would like to acknowledge the financial and technical support from managers and researchers at SINTEF, NOV, IRIS, and David Pixton. Their industrial viewpoints helped my research be more professional and practical.

Finally, I would like to give a special thanks to my wife, Jina, for her sacrifices to help me focus on my research and become a good husband and dad.

المنارة للاستشارات
www.manaraa.com

# TABLE OF CONTENTS

www.manaraa.com

المنارة للاستشارات
www.manaraa.com

# LIST OF TABLES

المنارة للاستشارات

www.manaraa.com

# LIST OF FIGURES

المنارة للاستشارات

www.manaraa.com

# NOMENCLATURE

| | |
|---|---|
| BHP | Bottom Hole Pressure |
| BHA | Bottom Hole Assembly |
| BPS | Bits per Second |
| CV | Controlled Variable |
| DV | Disturbance Variable |
| EKF | Extended Kalman Filter |
| HFM | High-fidelity Flow Model |
| IPOPT | Interior Point OPTimizer |
| LP | Linear Programming |
| LWD | Logging While Drilling |
| MWD | Measurement While Drilling |
| PWD | Pressure While Drilling |
| RCD | Rotating control Device |
| RSS | Rotary Steerable System |
| MD | Measured Depth |
| MPC | Model Predictive Control |
| MHE | Moving Horizon Estimation |
| MIMO | Multi-inputs and Multi-outputs |
| MPD | Managed Pressure Drilling |
| MPT | Mud Pulse Telemetry |
| MV | Manipulated Variable |
| SISO | Single-input and Single-output |
| NMPC | Nonlinear Model Predictive Control |
| NPT | Non Productive Time |
| PID | Proportional, Integral, and Derivative controller |
| QP | Quadratic Programming |
| ROP | Rate of Penetration |
| RPM | Rotations Per Minute |
| SFM | Simplified Flow Model |
| SP | Set Point |
| $SP_{hi}$ | Upper limit of the dead-band region of the $\ell_1$-norm objective function |
| $SP_{lo}$ | Lower limit of the dead-band region of the $\ell_1$-norm objective function |
| SPP | Stand Pipe Pressure |
| UKF | Unscented Kalman Filter |
| WDP | Wired Drill Pipe |
| WOB | Weight On Bit |

المنارة للاستشارات

www.manaraa.com

# CHAPTER 1. INTRODUCTION

Automation systems are increasingly important in many industries, especially those industries that need to reduce manual processes to improve efficiency, process economics, and reduce risk. In addition to improving safety and convenience, automation systems enable optimization strategies that are almost impossible to consistently apply by manual operation. The drilling industry has delayed automation longer than the downstream chemical processing industry because of limitations including inadequate measurements and manipulated variables that cannot be adjusted continuously. However, the rapidly changing crude oil market and desire to reduce operational variability and risk has renewed interest in drilling automation. This chapter introduces important drilling mechanisms and recent technical enhancements in drilling operations. The advanced control and estimation algorithms that are of interest to drilling operations are also discussed.

## 1.1 Oil and Gas Drilling Technology

Drilling technology has been implemented since ancient times, most commonly for the extraction of underground water resources. Drilling, once accomplished by man or animal power, has evolved into the large rigs that are prevalent today, an evolution that in large part was made possible by advances with the combustion engine. In modern drilling there are two established methods: cable-tool drilling and rotary drilling. Cable-tool drilling, invented earlier than rotary drilling, uses up and down motion of the rod with a sharp bit at the end of it. A relatively simple method, cable-tool drilling is still employed today, particularly for shallow oil wells. Alternately, rotary drilling uses rotation motion of the drill string to cut the rock formation with different types of drill bits and is the most popular choice for the oil and gas industry. It is a more complicated and efficient method than cable-tool drilling, enabling deeper and faster drilling. In addition to the advantages of rotary drilling, rotary drilling is also equipped with advanced technologies such as managed pressure drilling (MPD), directional drilling, and wired drill pipe (WDP). This chapter introduces

المنارة للاستشارات

www.manaraa.com

the main components of rotary drilling rigs and the functions of each component. In addition, it discusses MPD and WDP, two advanced technologies closely linked to drilling automation.

### 1.1.1 Overview of Rotary Drilling

The basic mechanism of the rotary drilling process is penetration into the rock formation by cutting the rock with a combination of downward force and rotating motion. This generates the fracture and frictional force between the drill bit and the surface of the rock. The rock cuttings are continuously transported to the surface by the drilling fluid (generally called drilling mud) circulation system. The main components of the rotary drilling rigs are divided into two parts: surface equipment and subsurface equipment. Surface equipment consists of a hoisting system, rotating system, and mud circulation system while subsurface equipment consists of a drill string and bottomhole assembly (BHA).

The power related to rotation, lifting, and mud circulation is generated and driven from the surface equipment. All the driving forces are transferred to the bottomhole through the drill string and mud. The hoisting system lifts up and lowers the drill string into and out of the borehole for purposes including pipe stand connection, bit replacement, and control of the drill string weight during normal drilling operations. A pipe connection procedure is necessary for extending the drill string and is accomplished by adding a new segment of drill pipe to the existing block as the drill deepens. Pipe connection takes place every 20 to 40 minutes depending on the rate of penetration (ROP). Drill bit replacement is not desired, but becomes necessary when a drill bit breaks or is otherwise damaged. Because the entire drill string has to be taken out to replace a broken bit, the non-productive time (NPT) is lengthened significantly by drill bit replacement. Unlike the first two functions of the hoisting system, controlling the weight of the drill string, called weight on bit (WOB), is a continuous part of regular drilling operations. The WOB is one of the important operation variables that can be adjusted by changing the hook load at the surface. On the other hand, the main function of the rotating system is to generate the rotation of the drill string and transfer the rotation to the drill bit at the desired revolutions per minute (RPM). The WOB and bottomhole RPM directly affect the ROP. Inadequately adjusted WOB and RPM can cause severe drilling problems by triggering vibration of the drill string. Drill string vibration can either badly affect the ROP or cause failure in the bit or drill string. The hoisting and rotating systems directly

المنارة للاستشارات
www.manaraa.com

impact the WOB and RPM, respectively. These relationships are classified as part of the drill string dynamics, whereas the mud circulation system is part of the drilling hydraulics. Drilling mud is a mixture of various chemical additives with water or oil that removes heat and cuttings from the bottomhole. It is fed by the mud pump from the surface, through the drill pipe, and sprayed out at the bottomhole through the bit nozzle. Mud carries the rock cuttings through the annulus up to the surface. The mud is regenerated at the mud pit by separating the cuttings and reconditioning the desired properties before it is recycled back down the drill string.

Beyond carrying rock cuttings, drilling mud serves to balance the formation pressure, transmit data via mud-pulse telemetry, and provide cooling and lubrication for the drill bit. The hydrostatic pressure and frictional pressure of the drilling mud ensure the pressure at the bottomhole, or more specifically the open hole area, is maintained higher than the formation pore pressure to block the influx of hydrocarbon gas into the borehole. This phenomenon of gas influx is commonly referred to as a gas kick. Hydrocarbon gas resulting from a kick has to subsequently be circulated out with heavier mud or stopped with a blowout preventer. Unsuccessful control of the gas kick can cause a catastrophic blow-out. Formation fracture pressure and collapse pressure profiles also exist above and further below the pore pressure, respectively. For conventional 'overbalanced drilling', the bottomhole pressure (BHP) should be maintained between the pore pressure and fracture pressure to block the formation gas entering into the wellbore. Conversely, more recently developed 'underbalanced drilling' can be implemented, wherein gas influx is intentionally allowed by maintaining the BHP lower than pore pressure. A multi-phase separator at the surface recovers the hydrocarbon fluid from the mud. The acceptable pressure range, normally for overbalanced drilling, is called the 'drilling window'. The other important function of drilling mud is to transmit bottomhole data such as pressure, temperature, and information related to the drill string dynamics and directional drilling. In this data transmitting system, called mud-pulse telemetry (MPT), the mud acts as a medium for the pulse signals that are generated from the bottomhole.

Subsurface equipment consists of two important parts. First is the upper drill string that is an assembled collection of drill pipes, and second is the lower section of drill string referred as the BHA. The BHA includes the drill bit at the end as well as the sensor packages and devices for directional drilling such as a Rotary Steerable system (RSS). The BHA is the heaviest section of the drill string and provides the required WOB for generating downward force.

المنارة للاستشارات
www.manaraa.com

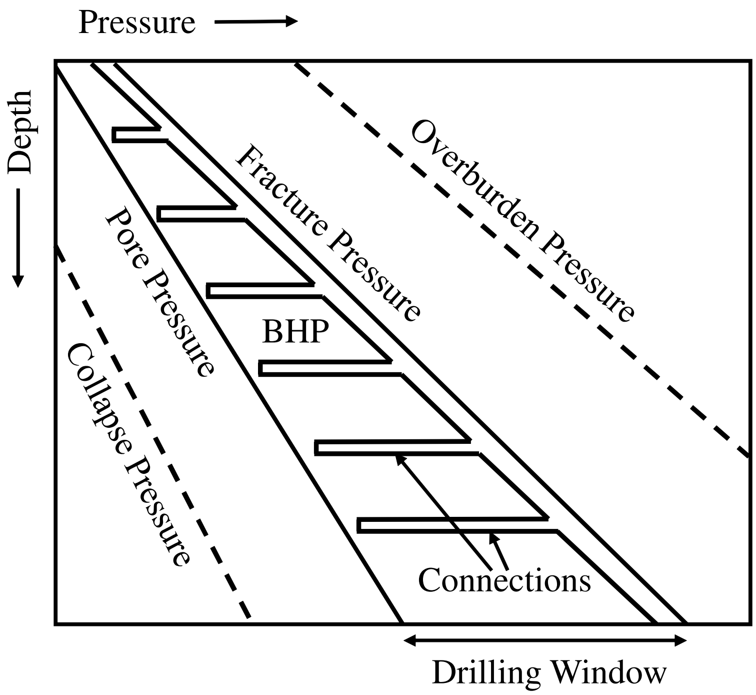

Figure 1.1: Schematic representation of drilling window

### 1.1.2 Managed Pressure Drilling

BHP regulation is critical for drilling in many formations. As briefly mentioned in the previous section, BHP should be maintained within the drilling window to prevent drilling problems (Figure 1.1). For example, if the BHP drops below the pore pressure, gas may enter into the wellbore from the formation, causing a gas kick that often requires drilling operations to be suspended to circulate out the gas. The gas influx can evolve into a catastrophic ‘blow out’ when it is not treated properly. If the downhole pressure drops further, the well wall may collapse, leading to a stuck drill string that is held in place by formation fragments. On the other hand, if the downhole pressure exceeds the fracture pressure, a significant amount of mud may escape into the formation, increasing the operating cost for replenishing the mud. Lost circulation material or additional casing maybe introduced to plug the fractured reservoir. If the downhole pressure increases above the overburden pressure, the formation will be damaged by formation fracture.

In a conventional drilling system, there are two variables to control the BHP: mud density and mud flow rate. However, because the wellbore is open to the atmosphere at the surface, it is

المنارة للاستشارات

www.manaraa.com

hard to achieve precise BHP control by adjusting only these two variables. Dynamic BHP, which refers to the BHP when the mud is circulating, is a summation of the hydrostatic pressure of mud column and the frictional pressure of the mud flow. Static BHP refers only to the hydrostatic pressure when the mud is not circulating, which regularly occurs for pipe connection. In general, the mud density is kept constant until the either the dynamic or static BHP get close to the fracture pressure or pore pressure, respectively. (Figure 1.2).

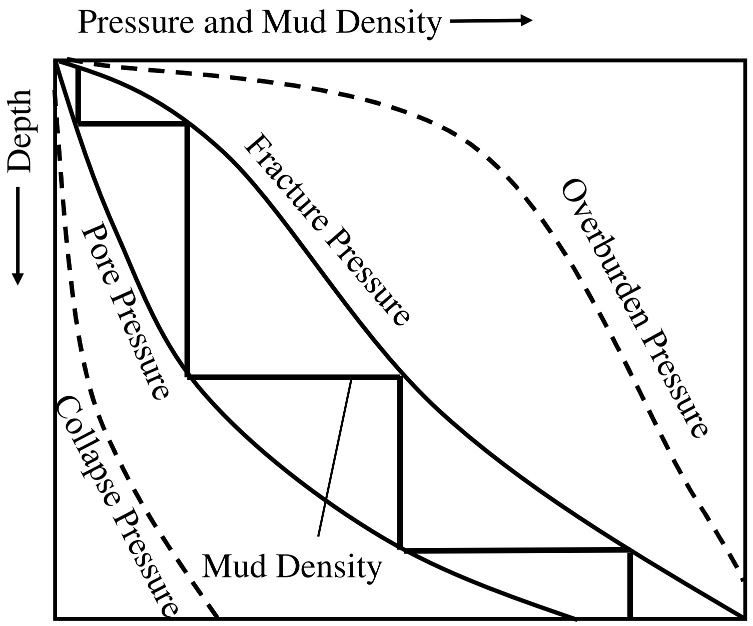

Figure 1.2: Wide drilling window

For wells with a conventional drilling system that have a narrow drilling window (Figure 1.3) (normally deepwater wells) BHP control is more demanding because the mud density frequently changes, as observed in Figure 1.3, and every density adjustment requires a stop in drilling that lengthens the NPT. Furthermore, such systems do not have the means to control kick without stopping the mud circulation, which adds to the NPT. These systems do not have enough of a pressure margin between dynamic and static BHP when pipe connection occurs, described in Figure 1.1 as bumps in the BHP plot.

www.manaraa.com

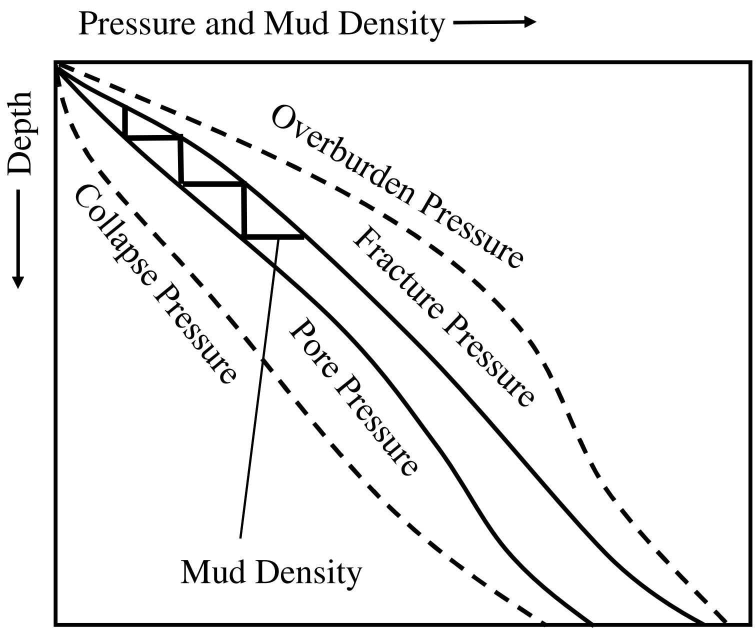

Figure 1.3: Narrow drilling window

In a MPD system, the wellbore is completely isolated from the atmosphere by the rotating control device (RCD) and the mud return flow is routed to the choke manifold (Figure 1.4). This choke valve improves the BHP control significantly enabling the fast and precise pressure control without stopping the drilling. Aside from the choke manifold system, another option for improved MPD is the back pressure pump. The back pressure pump recirculates the mud from the mud pit to the choke valve inlet to generate more annulus pressure by adding more annular flow. The back pressure pump is usually activated to compensate for the frictional pressure when the mud circulation stops for pipe connection, which removes the pressure difference present during normal drilling. Thus, MPD opens the door to implementation of an automated BHP control system while providing a rich array of challenges for control and automation applications using hydraulic models and simulators [1–7].

### 1.1.3 Wired Drill Pipe

Increasing demands of petroleum resources have driven the oil and gas industries to explore more challenging reservoirs such as deepwater reservoirs that have narrow drilling windows. Also, the evolution of horizontal drilling requires more sophisticated path control in terms of directional

المنارة للاستشارات
www.manaraa.com

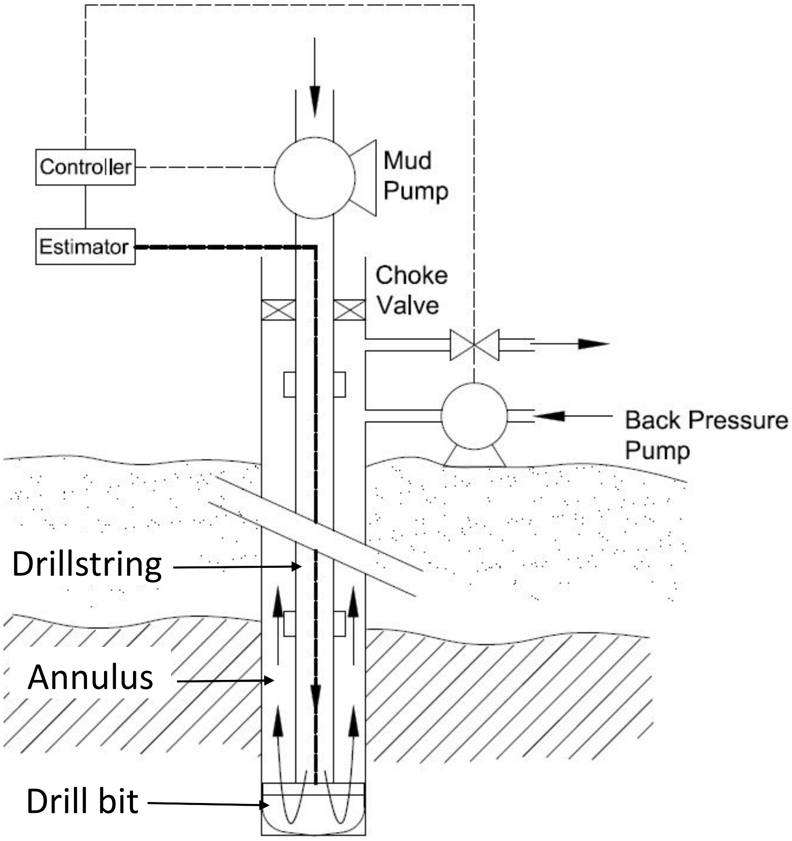

Figure 1.4: Schematic of the Automated MPD System [8]

drilling. The improved data communication between bottomhole tools and surface crews or equipment is the most crucial factor to achieve the accessibility to these reservoirs. MPT is an existing method of data transmission which is being replaced by WDP [9]. MPT uses the pulse signals generated by the opening and closing movement of valves in the drill string. This up and down movement of mud flow results in a pressure pulse. This pressure pulse signal travels through the mud to either the surface or bottomhole with different patterns that are captured and interpreted by the surface device or bottomhole tools, respectively. The average data communication speed of MPT is about 5-10 BPS [10] which is not sufficient for configuring a real-time automation system. Moreover, because the mud plays a role as a medium of the signal transmission, it limits the data availability and makes it complicated to interpret the pulse signal when the mud does not circulate or when mud of multiple properties is combined in the well.

المنارة للاستشارات
www.manaraa.com

When using a WDP system, the data transmission rate is dramatically increased by up to $10^5$ BPS [11,12]. WDP technology provides two-way and high-speed measurements from the bottomhole and intermediary string sensors that enable more appropriate decision making regardless of the level of mud circulation.

## 1.2 Model Based Control and Estimation

This section focuses on model predictive control (MPC) and moving horizon estimation (MHE) algorithms for BHP regulation. The principles and advanced features of MPC and MHE algorithms are presented and explored.

### 1.2.1 Model Predictive Control

MPC algorithms have been successfully implemented in many industries since the introduction of MPC in the early 1970s. It has many advanced features over a traditional PID controller. MPC predicts the future behavior of the process by evaluating the process model at the current time step. The benefit of this prediction feature is that it can correct the process input variables in advance by looking at the future status of the process. While PID control has a similar feature, it is employed in an indirect manner that does not involve the process model in the online implementation. The MPC prediction refers the past movements of the input variables for prediction, and updates the prediction error detected at the current step to the prediction. These make the MPC prediction more robust under some degrees of model mismatch or unmeasured process disturbances. Additionally, MPC can manage multiple variables simultaneously, called Multiple Inputs and Multiple Outputs (MIMO) control. MPC can naturally handle the MIMO control by setting up the multiple terms in the Quadratic Programming (QP) objective function. Therefore, MPC distributes the control burden into multiple process input variables that have a relationship to the control objective. This MIMO control feature is difficult to equip using multiple Single Input and Single Output (SISO) controllers, such as PID controllers, because complexity is added by the need for additional calculation blocks to decouple the interactions between variables. Furthermore, process optimization strategies can be embedded into the MPC by adding Linear Programming (LP) terms in the objective function. This drives the process to a more beneficial state.

المنارة للاستشارات
www.manaraa.com

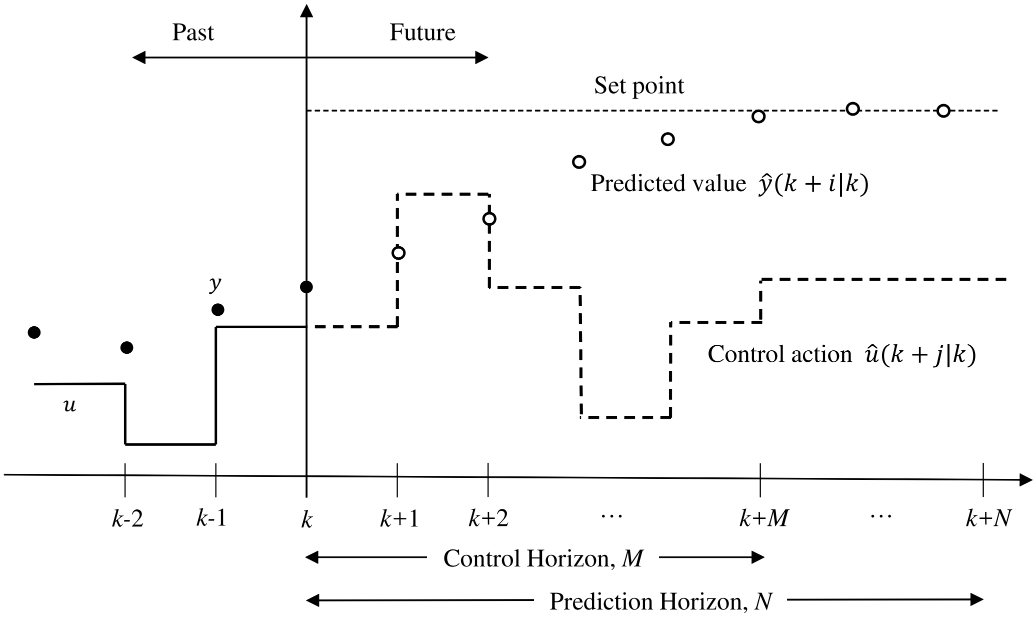

Figure 1.5: Schematic illustration of receding horizon concept of MPC

### 1.2.2 Moving Horizon Estimation

As model-based control and optimization strategies receive more attention in many industries, the estimation of unknown or uncertain parameters is necessary to maximize the benefit of an automated system. Estimators generally estimate the current state of the process when data is not measurable or the sensors are not reliable, as is the case with real-time quality estimation in distillation columns when the on-line quality analyzers are not available. An estimator also estimates the unmeasured variables or parameters in the model that is being used by MPC. As a result, the control performance can be improved by increasing the accuracy of the MPC. There are many different types of estimation algorithms including MHE, the Extended Kalman Filter (EKF) and the Unscented Kalman Filter (UKF) [13, 14]. Various types of estimators are reviewed and compared in [15].

MHE is functionally similar to MPC and constitutes the most capable estimation algorithm [16–18]. It calculates unknown parameters by solving the QP objective function which includes primarily the model errors. The objective function of MHE includes the past measurements and model results while the MPC projects the model and drives to a setpoint. In drilling automation

www.manaraa.com

research, estimation algorithms are tuned to detect certain events such as unexpected gas influx or buildup of cuttings within particular sections of the annulus. Various types of Kalman filters have previously been investigated for estimating the unknown parameters in drilling operations [19]. Previous research also uses a combination of EKF and MHE to estimate the density and gas influx flow rate [20,21] using a squared error objective function to penalize deviation of the model values from available measurements. Estimators for underbalanced drilling have also been designed using MHE and UKF [22,23].

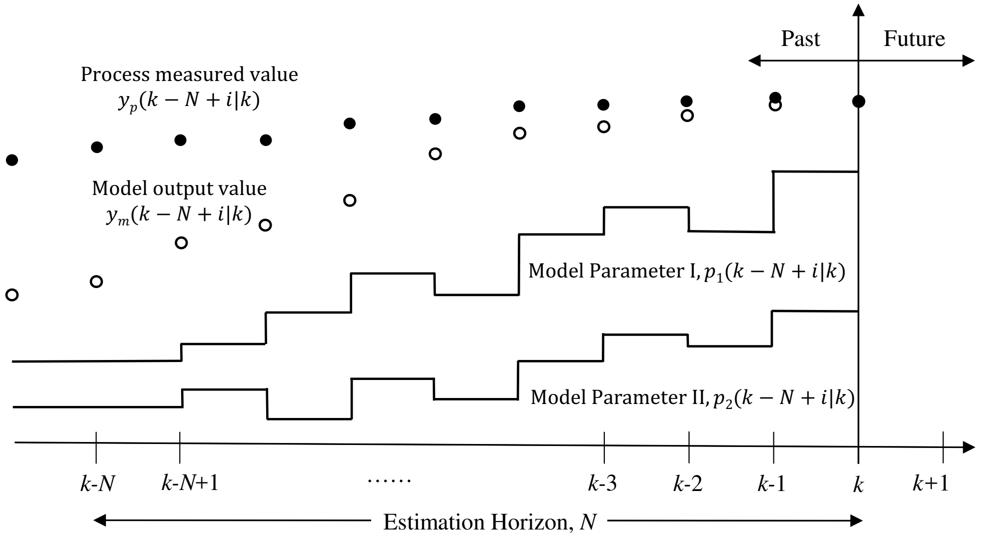

Figure 1.6: Schematic illustration of receding horizon concept of MHE

## 1.3 Research Objective

Many industries have successfully adopted linear MPC [24,25]. However, these processes have either semi-batch characteristics or nonlinear behavior, thereby limiting the potential application of linear MPC. The drilling process is inherently nonlinear because the operations include a wide range of dynamic input to output relationships that are not linear. In addition, because the operation stops and starts periodically, the portion of time that the process goes through a transient state is not insignificant. Several studies show that the performance of a linear MPC controller for the drilling process is good in a limited operation regime [26–28]. However, linear MPC also exhibits severe limitations when moving to another operation regime outside the range of the training

www.manaraa.com

data [26–28]. There are another group of studies that attempt to apply a nonlinear MPC algorithm for drilling [21, 29–31]. These studies develop and employ a low-order model to improve the computational speed of NMPC. Several low-order model equations for drilling automation are described in previous research [6, 32–37]. A low-order model is more feasible to use for real-time control purposes because it requires less computational time than high-fidelity simulators by simplifying the dynamics of the drilling process. The accuracy of a low-order model is verified by comparison with data from a physical drilling test rig [4]. The verification data includes pressure hydraulics, ROP, friction factor, drill string dynamics, and WOB dynamics.

The objective of this study is to develop an automation system for MPD. MPD has the potential to benefit from MPC and MHE algorithm that has already been proven in a number of industries. The MPC and MHE in this study use the different types of models. One is a Simplified Flow Model (SFM), developed by SINTEF, and the other is a Hammerstein-Wiener model. SFM is a simplified version of SINTEF's High-fidelity Flow Model (HFM), created by simplifying or removing complex dynamics that have a limited effect on the drilling hydraulics calculations. It retains the same accuracy of the HFM for hydraulics calculation which must be more precise than the existing low-order model and have improved computational speed and stability than HFM. The Hammerstein-Wiener model is an empirical type of nonlinear model that contains the linear dynamics blocks and static nonlinear blocks separately.

Two different high-fidelity drilling simulators are used for verifying the performance of the MPC and MHE. The first is WeMod, developed by the International Research Institute of Stavanger (IRIS), and the second is the HFM developed by SINTEF. These high-fidelity drilling simulators use a dynamic model that describes a one-dimensional, two-phase flow in pipelines with nonlinear partial differential equations (PDEs). The PDEs describe mass, momentum, and energy balances for each phase. The momentum equations combine to form a drift-flux formulation. Models of friction, velocity, temperature, gelling, and flow regime simulate the virtual well system [38]. For solving the nonlinear optimization problems, APMonitor optimization suite [39] and Sequential Least Squares Programming (SLSQP) module in a Python SciPy function are used. This automation system seeks to maximize the rate of penetration (ROP) and regulate the BHP. This study verifies the performance of nonlinear model predictive control (NMPC) for both normal drilling and drilling during abnormal conditions.

المنارة للاستشارات
www.manaraa.com

## 1.4 Outline

The dissertation is outlined in three successive chapters as follows:

**Chapter 2** presents a new simplified flow model (SFM) for BHP regulation in MPD operations. The SFM is embedded into model based control and estimation algorithms that use MPC and MHE, respectively. BHP control performance is evaluated in scenarios of drilling, pipe connection, and mud density displacement and the efficacy of the SFM is tested in control schemes applicable to both WDP and mud pulsing. A trusted high-fidelity flow model (HFM) is used to simulate well conditions that are used to evaluate performance of the controller using the SFM.

**Chapter 3** demonstrates a new Hammerstein-Wiener NMPC for BHP regulation in drilling. Hammerstein-Wiener models employ input and output nonlinear static blocks before and after linear dynamics blocks and thereby simplify the controller design. The control performance is evaluated in scenarios of drilling, pipe connection, and kick attenuation. A physics-based drilling simulator, WeMod, is used for model identification and control performance evaluation.

**Chapter 4** is a brief summary of the conclusions and future work.

## 1.5 Contributions

- Developed MPC and MHE for the MPD process using newly developed SFM in Chapter 2.
- Calibrated frictional pressure loss in the drill string and annulus using SFM MHE in Chapter 2.
- Evaluated the BHP control performance MPC and MHE using an SFM for semi-closed loop and full-closed loop configurations in Chapter 2.
- Applied Hammerstein-Wiener empirical non-linear model for MPC for BHP control in Chapter 3.
- Evaluated the BHP control performance of Hammerstein-Wiener MPC for the MPD operation with WDP system in Chapter 3.
- Performed case studies for typical normal and abnormal operation scenarios in drilling operation such as drilling, pipe connection, kick attenuation, and mud density displacement in Chapters 2 and 3.

المنارة للاستشارات
www.manaraa.com

- Investigated model mismatch between SFM and HFM in Chapter 2.
- Investigated non-linearities in drilling operation in Chapter 3.
- Compared control performance between conventional PID and Hammerstein-Wiener MPC in Chapter 3.
- Developed the MPC variable switching algorithm for the kick attenuation control in Chapter 3.

## 1.6 Publications

The main contributions to this thesis were presented in the following conference papers:

- **Park, J.**, Price, C., Pixton, D.S., Hedengren, J. D., Aghito, M., Nybø, R., & Bjørkevoll, K. (2018). Model Predictive Control and Estimation of Managed Pressure Drilling. Control Engineering Practice. (Submitted)
- **Park, J.**, Webber, T., Shishavan, R. A., & Hedengren, J. D. (2017). Improved Bottomhole Pressure Control with Wired Drillpipe and Physics-Based Models. In SPE/IADC Drilling Conference and Exhibition. Society of Petroleum Engineers. doi:10.2118/184610-MS

المنارة للاستشارات
www.manaraa.com

# CHAPTER 2. SIMPLIFIED FLOW MODEL VALIDATION FOR BOTTOMHOLE PRESSURE REGULATION OF MANAGED PRESSURE DRILLING

## 2.1 Introduction

Drilling automation has the potential to improve operational efficiency, safety, and environmental impact of well manufacturing. Implementation of drilling automation leads to two important considerations, that of the drill string dynamics, and that of the system hydraulics. The primary objective of automation regarding the drill string dynamics is to reduce the vibrations of the drill string and maximize the energy transferred for cutting rock. Minimization of drill string vibrations preserves that energy and yields more efficient operation. Regarding system hydraulics, the primary objective of automation is to control the bottomhole pressure (BHP). Such control may be accomplished by using drilling fluid to maintain a specified BHP. BHP regulation is crucial because drilling rate of penetration (ROP) improves with a lower BHP that approaches the lower pore pressure limit [40]. Varying methods, challenges, and benefits of BHP control are addressed in this paper. By managing the pressure within the drilling window, mud loss to the formation can be reduced and lower the risk of gas influx from the formation. With fine control for BHP, wells with narrow pressure margins become more readily accessible. Although these two parts of drilling automation research usually are evolving separately, they should be integrated into a single research topic in the future when their technologies are mature. Asgharzadeh et al. [20] investigated ROP optimization combined with BHP control considering the mutual effects of the drill string dynamics and hydraulics. MPC is an advanced control algorithm that has been successfully implemented in a variety of industries [24]. Many attempts have been made to successfully apply MPC to managed pressure drilling (MPD) operation. However, there are several inherent challenges in drilling operation that inhibit use of full closed-loop control. The most apparent obstacle is the lack of a real-time downhole pressure measurement. Measurement while drilling (MWD) is a common way to collect BHP measurements. However, low bandwidth of the MWD is not sufficient for a

المنارة للاستشارات
www.manaraa.com

real-time feedback signal, and the pressure wave that serves as the medium for signal transmission generates considerable delay [37]. The delay time varies with the well depth and is vulnerable to pressure fluctuations caused by the choke manifold. A modern high-speed telemetry system, WDP, is the only current physical solution that removes these data transmission issues [41]. Despite increasing interest in WDP, most wells continue to use MWD for lower costs and proven field experience compared to WDP. A second challenge faced by drilling automation is the difficulty of modeling the physical characteristics of the drilling process and employing real-time predictions in the control system. High-fidelity flow models (HFM) have been commonly used for understanding operation conditions and decision making. However, the complexity and a large number of input variables in HFM make them unsuitable for use in a real-time control system. Thus, many MPD automation research studies have attempted to employ reduced order models which capture the primary dynamics of the drilling process [28,32,33,37]. However, the inevitably compromised accuracy of the simplified models shows a discrepancy between actual operation and model results. This model mismatch becomes more prominent in transient periods caused by operational changes than a steady state. Park et al. [42] applied Hammerstein-Wiener non-linear empirical model and Eaton et al. (2017) [8] developed a model switching control method to improve the BHP control performance under the existing obstacles. Landet et al. (2013) [43] investigated the MPC automation for offshore rig having the heave-induced pressure fluctuations. In this study, newly developed SFM (SINTEF) is used for BHP pressure control and compare the results between non-WDP rig and WDP rig.

## 2.2 Simplified Flow Model

A SFM for real-time hydraulic calculations in drilling operations was recently proposed in [44]. The SFM is based on the background technology provided by a HFM which has been employed in many applications, including choke control in several successful MPD operations where accurate pressure control was achieved [24,37,41]. The calculations are based on discretization of the well volume and a numerical solver for the mass and momentum conservation equations the govern the physics of the well. One possible limitation when using advanced high-fidelity models in drilling automation is that these models are comprehensive, require to be configured, monitored and tuned by an expert, and it is hard to eliminate fully the risk of running into numerical insta-

المنارة للاستشارات
www.manaraa.com

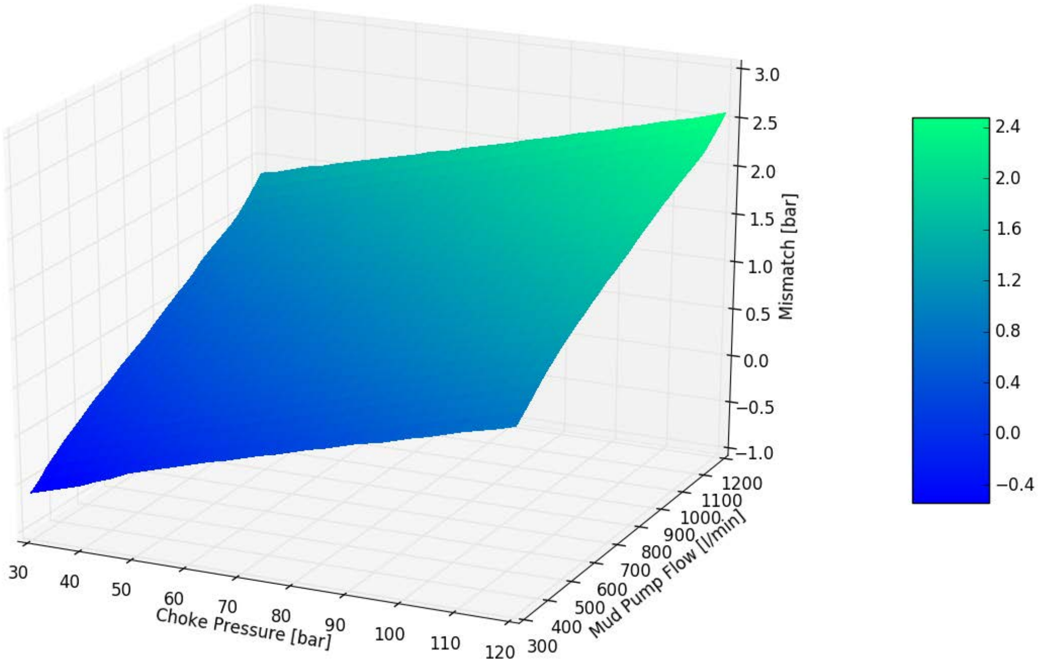

Figure 2.1: Difference between steady state BHP output from HFM and SFM to identify model mismatch at varying conditions

bilities. This motivated the development of the SFM, which is significantly simpler, faster, and more robust than the HFM, but retains much of the accuracy of the HFM. Figure 2.1 shows the model mismatch between HFM and SFM in varying conditions. The SFM is a dynamic model, as the HFM. Mass transport calculations include dynamic effects in that e.g. an increase in pressure causes a delay in flow out due to compression of the fluid in the well. However, accuracy during the transient phases is relaxed somewhat in the simplified model to allow calculations to be done with a minimum of numerical iterations. Another simplification is to keep temperature profile fixed, rather than doing the dynamic temperature calculation that many high-fidelity models can do. This simplification is acceptable because changes in temperature profile normally goes much slower than rapid changes in the pressure profile due to operational changes, and therefore a good tuning algorithm can be used to take care of the slowly drifting consequences of temperature changes. Some additional simplifications are made in sub-models to reduce need for numerical iterations, for example the rheology model. The HFM fits rheology data to a Herschel Bulkley model, while

المنارة للاستشارات
www.manaraa.com

the SFM utilize the linear Bingham model. Still calculations are relatively sophisticated, and include for example pressure and temperature dependent fluid properties, with density either from published correlations or from input tables of laboratory data. The SFM is therefore much faster and robust than the HFM, and at the same time more accurate than existing lower order model therefore it is recommended for integration in advanced control system methods such as MPC and MHE.

## 2.3 System Configurations

Control system architecture for MPD automation varies according to the availability of BHP data. Several potential architectures are portrayed in Figures 2.2, 2.3 and 2.4. They display block diagrams of the signal chains for each architecture. Note that dashed lines in these figures represent the input signals of the controller that are computed from hydraulic models. If the BHP measurements are available for the control system, a solid line represents the path of measured data. Figure 2.2 shows an *open loop* configuration wherein the control system relies on the calculated BHP of the SFM and no actual bottomhole data is fed into the control system. This is the most passive method of automating the system, where automatic control decisions are not directly fed into the rig equipment controllers, but are initially screened by operators in an open-loop manual mode. This therefore constitutes an advisory system.

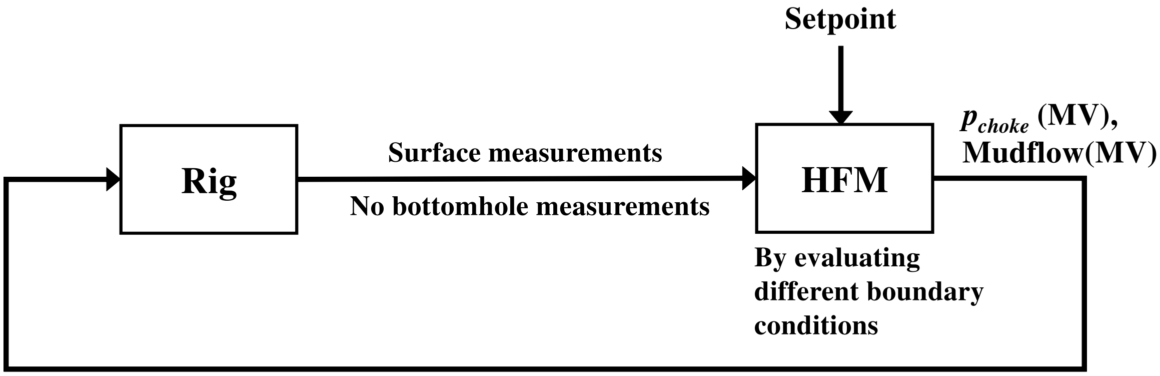

Figure 2.2: Open loop control configuration - Advisory system

www.manaraa.com

Figure 2.3 represents a *semi-closed loop* configuration, which is a common configuration in MPD automation research especially when WDP is not available [45–47]. Instead of fully relying on a model calculation (e.g., Figure 2.2), methods are introduced in this configuration to estimate the BHP from surface measurements. Moving horizon estimation is the estimation method presented in this paper but is only one of a number of useful estimation methods. In this scenario the moving horizon estimator (MHE) acts as a soft sensor that infers the BHP by processing the surface measurements through the SFM. Unlike the open loop configuration of Figure 2.2, the MHE minimizes model mismatch by dynamic optimization of certain unmeasured drilling parameters, such as mud density and friction factor. Furthermore, the model may be occasionally updated or tuned by periodic downhole measurements (e.g., via mud pulse telemetry) to increase accuracy.

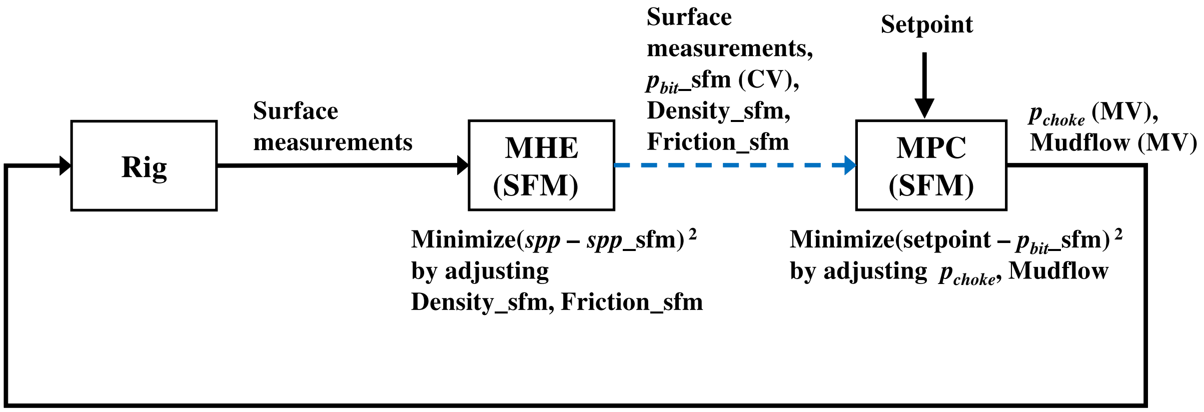
Rig
Surface measurements
MHE (SFM)
Surface measurements, $p_{bit}$_sfm (CV), Density_sfm, Friction_sfm
Setpoint
MPC (SFM)
$p_{choke}$ (MV), Mudflow (MV)
Minimize(*spp* – *spp*_sfm)$^2$ by adjusting Density_sfm, Friction_sfm
Minimize(setpoint – $p_{bit}$_sfm)$^2$ by adjusting $p_{choke}$, Mudflow

Figure 2.3: Semi-Closed loop control configuration - Moving horizon estimator

Finally, if real-time BHP measurements are available, a *full-closed loop* configuration may be employed. This type of system is presented in Figure 2.4. Note that, even though bottom hole measurements are available in real time, an estimator is still present in this configuration, since it is needed to estimate unmeasured drilling parameters such as mud density or friction factor. Because actual BHP measurements are used in the MHE calculation, the resulting estimated quantities are more reliable than those of the semi-closed loop case in Figure 2.3. The SFM is continuously updated with the estimated parameters to increase the accuracy and reliability of the controller. We note here that, while various telemetry systems can supply real time BHP measurements, varying quality and quantity of real-time data are available from these different schemes. While mud pulse

المنارة للاستشارات
www.manaraa.com

telemetry can provide real-time data, this data is subject to transmission delays on the order of at least a few seconds and delivery of the data may be subject to deprioritization depending on what other data is occupying the limited transmission channel. Of course, mud pulse telemetry ceases when mud pumps are shut off. These factors introduce uncertainty into the control process and place more reliance on model-based estimates. High-speed telemetry provided by wired drill pipe overcomes these limitations and provides more timely and abundant data for full closed loop control.

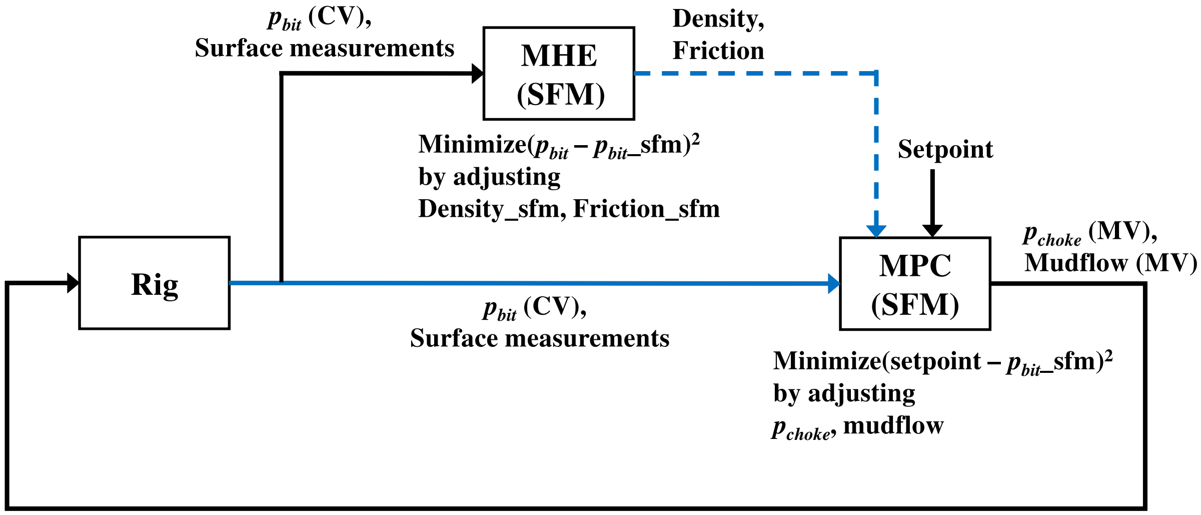

Figure 2.4: Full-Closed loop control configuration - Moving horizon estimator

## 2.4 Model Based Control and Estimation

There are several steps in the MPC calculation. First, it predicts the future behavior of the process by evaluating the process model (in this case the SFM) at the current time step. The benefit of this prediction feature is that it can correct the process input variables in advance by looking at the future status of the process. Second, it determines the sum of squared error between the setpoint trajectory and model prediction values throughout the prediction horizon. Third, it performs the control calculation by solving the dynamic optimization problem to find the optimal sequences of process inputs (MVs). The first value of the MV sequence is applied to the process and repeats the entire cycle for every time step.

www.manaraa.com

The MHE algorithm shares this main concept with MPC. It calculates the unknown parameters in the model by solving the Quadratic Programming (QP) objective function that mainly includes the model errors. The objective function of MHE refers the past data of measurements and model results while the MPC refers the future model prediction and setpoint. The QP objective functions used in this study are the squared error objective. The objective functions associated with MHE and MPC are shown in Equations (2.1) and (2.6), and the parameter descriptions are shown in Table 2.2 and 2.1, respectively.

$$\min_{\Delta p}\Phi = \sum_{i=1}^{N}[(y_{p,k-N+i|k} - y_{m,k-N+i|k})^T W(y_{p,k-N+i|k} - y_{m,k-N+i|k}) + (\Delta p^T_{k-N+i|k} V \Delta p_{k-N+i|k})] \tag{2.1}$$

$$where, \Delta p_{k-N+i|k} = p_{k-N+i|k} - p_{k-N+i-1|k} \tag{2.2}$$

$$s.t. \;\; 0 = f(\dot{x}, x, y, p, d, u) \tag{2.3}$$

$$0 = g(x, y, p, d, u) \tag{2.4}$$

$$0 \leq h(x, y, p, d, u) \tag{2.5}$$

Table 2.1: Summary of parameters used in QP objective function for MHE

| **Parameter** | **Description** |
|---|---|
| $\Phi$ | Objective function |
| $N$ | Horizon length for MHE |
| $k$ | Current time step |
| $y_p, y_m$ | Measured CV value ($y_p$) and model result of CV value ($y_m$) |
| $V, W$ | Weighting Matrices for CVs and parameters |
| $u, x, p, d$ | Model inputs($u$), states($x$), parameters($p$), and disturbance($d$) |
| $f, g, h$ | Model equation ($f$), output function ($g$), and inequality constraints ($h$) |

المنارة للاستشارات
www.manaraa.com

$$\min_{\Delta u}\Phi = \sum_{i=1}^{N}[(\hat{y}_{k+i|k}-\hat{y}_t)^T Q(\hat{y}_{k+i|k}-\hat{y}_t)] + \sum_{j=1}^{M}(\Delta u_{k+j|k}^T R \Delta u_{k+j|k}) \tag{2.6}$$

$$where, \Delta u_{k+j|k} = u_{k+j+1|k} - u_{k+j|k} \tag{2.7}$$

$$s.t. \;\; 0 = f(\dot{x}, x, y, p, d, u) \tag{2.8}$$

$$0 = g(x, y, p, d, u) \tag{2.9}$$

$$0 \leq h(x, y, p, d, u) \tag{2.10}$$

$$\tau_c \frac{dy_t}{dt} + y_t = sp \tag{2.11}$$

Table 2.2: Summary of parameters used in QP objective function for MPC

| Parameter | Description |
|---|---|
| $\Phi$ | Objective function |
| $N, M$ | Prediction horizon($N$), Control horizon($M$) |
| $k$ | Current time step |
| $\hat{y}$ | Predicted CV value of dynamic model |
| $\hat{y}_t$ | Desired set point trajectory in the prediction horizon |
| $Q, R$ | Weighting Matrices for CVs and MVs |
| $sp$ | Set point in the prediction horizon |
| $u, x, p, d$ | Model inputs($u$), states($x$), parameters($p$), and disturbance($d$) |
| $f, g, h$ | Model equation ($f$), output function ($g$), and inequality constraints ($h$) |
| $\tau_c$ | Time constant of desired controlled variable response |

## 2.5 Case Studies

Well conditions are simulated in this study by a high-fidelity flow model that has been shown through field experience to accurately represent field conditions in the tested regime. This study shows that tight pressure control can be maintained during the tested procedures when the controller and estimator are based on a nonlinear physics-based simplified model of the process. While this study is specific to the geometrical and physical constraints of the managed pressure drilling environment, the approach employed is extensible to applications in other industries where

المنارة للاستشارات
www.manaraa.com

a similarly simplified model may be used in conjunction with moving horizon estimation and model predictive control.

Well simulation studies have been used to assess the behavior of a control system employing the new SFM. In these studies, the SFM provides simulation data to MPC and MHE routines, and thereby helps assess the impact of adjusting choke valve pressure and drilling fluid flow on the controllers ability to keep BHP within established target limits. The field-tested HFM mentioned previously simulated well conditions in lieu of field data. A vertical well profile was selected for all simulations; other relevant well model parameters are presented in Table 2.3.

Both semi-closed loop and full-closed loop control schemes were tested under the following four scenarios:

1. a model calibration (to provide a basis for subsequent scenarios),
2. BHP control and simultaneous parameter estimation under normal drilling conditions (flow, drillstring rotation, formation penetration),
3. a pipe connection including cessation of flow and rotation, and
4. mud density displacement over a fixed period of time.

Scenario 1 simply ensures convergence of the SFM results with measured well conditions. The remaining scenarios provide different challenges to a controller that are expected in a managed pressure drilling environment.

In all case study scenarios, the two control system configurations are investigated and compared. Semi-closed loop configuration emulates the case where the BHP measurements are not reliable. Thus, the stand pipe pressure (SPP) measured from the surface is used for BHP estimation. On the other hand, the full-closed loop configuration simulates a rig where reliable BHP measurements can be used for MHE and MPC. The detailed descriptions of the scenarios are presented in following subsections.

المنارة للاستشارات
www.manaraa.com

Table 2.3: Wellbore Conditions I

| **Parameter** | **Value (AES)** | **Value (SI)** |
|---|---|---|
| Well depth | 12,349 ft | 3,764 m |
| Riser inner diameter | 9.66 in | 0.25 m |
| Water depth | 731.6 ft | 223 m |
| Casing inner diameter | 8.5in | 0.22 m |
| Casing depth | 12,349 ft | 3,764 m |
| Drill string average outer diameter | 4.5” | 0.12 m |
| Pore pressure | 1.33 ECD | 1.33 ECD |
| Fracture pressure | 1.927 ECD | 1.927 ECD |
| Initial mud density | 1.49 s.g. | 1.49 s.g. |
| Mud temperature | 122 F | 50 °C |

### 2.5.1 Model Calibration

Using MHE in model calibration leads to the minimization of mismatch between the simplified model and the actual conditions (represented in this case by the HFM). When assuming mud pulse communication between the surface and the bit downhole the sparsity and irregularity of data must be addressed. The MHE relies not on the actual bit pressure, but on the measured standpipe pressure as this is a measurement that can be reliably collected for estimation. This works under the assumption that changes in the bit pressure and changes in the standpipe pressure will occur nearly concurrently and that they are correlated. However, while the two measurements do move concurrently, the relationship is not constant due to frictional pressure loss at various flows. Therefore, when the standpipe pressure is used for estimation over large ranges of choke pressure and mud flow, the mismatch between the actual BHP and the SFM BHP increases. Minimization of the mismatch is accomplished by model calibration as downhole measurements become available. If WDP is used, the estimation would rely directly on the BHP measurements as they compare the simulated BHP measurements. Thus, periodic calibration would not be necessary as the model would be continuously calibrated because of the direct use of BHP measurements.

المنارة للاستشارات
www.manaraa.com

### 2.5.2 Normal Drilling

As previously stated, BHP control provides the ability to drill in narrow pressure wells in addition to optimizing ROP. In a normal drilling scenario both manipulated variables (choke pressure and drilling fluid flow) are available for manipulation by the controller. Assuming the friction factors are properly calibrated in the model by the model calibration procedure, the MPC algorithm minimizes the difference between the set point and the calculated BHP across the prediction horizon and accurately drives the BHP to the set point while submitting to provided manipulated variable constraints, such as the maximum rate of opening or closing for the choke valve or the allowable ramp rate for the mud pump.

### 2.5.3 Pipe Connection

During a pipe connection procedure, the normal control processes must be modified to accommodate the addition of more pipe. As the drill bit deepens during the drilling process additional pipe lengths are periodically added to the drill string. The addition of pipe is typically required every one to three hours [46] but is ultimately dependent on the pipe stand length and the ROP. During this pipe connection it is necessary to ramp the drilling fluid flow rate to zero, attach the new pipe length, and then bring the flow rate back up to normal conditions again. Thus, the mud flow rate changes from an optimized output of the controller to a set input that steadily ramps down to zero. As the mud flow rate is brought to zero the controller then relies solely on the choke pressure until the pipe connection is complete. However, because pipe connection is a planned event and the ramp rate is known in advance, the ramp rate can be passed into the MPC so that the changing mud flow can be considered in the BHP predictions of the MPC and improve control accuracy during the pipe connection period.

### 2.5.4 Mud Density Displacement

At the end of the MPD operation it is desired to shut off the choke valve. To reduce reliance on the choke pressure in the control scheme higher density mud is fed to the bottom hole. This higher density mud essentially serves as a less accurate substitute for the choke valve because it exerts higher pressure on the open hole so that the choke manifold can be released and disengaged

www.manaraa.com

from BHP management. In this scenario, the mud density changes over a period, thus allowing for a slow opening of the choke valve. As the density changes, the controller accounts for this change in system dynamics as it manages the BHP. This scenario differs from the pipe connection scenario in that the controller adjusts to rely solely on the drilling fluid flow, whereas for pipe connection the drilling fluid flow must be ramped down. Throughout the period of density transition and choke valve ramp up, the estimator is relied upon to provide accurate friction factors that keep the model accurate despite the changing conditions.

## 2.6 Results and Discussions

This section presents the results of model calibration, normal drilling, pipe connection, and mud density displacement case studies. The control performances of semi-closed loop and full-closed loop configurations are compared for the latter three scenarios.

### 2.6.1 Model Calibration

Figure 2.5 presents the results of MHE to calibrate the annulus and drill string friction factors in normal drilling conditions. These results are observed using a prediction horizon of 25 seconds. The estimator first estimates the annulus friction factor ($f_a$) at 150 seconds which aligns the calculated BHP with the actual BHP as presented by the HFM simulation. At 400 seconds the estimator calculates the drill string friction factor ($f_d$), which causes the calculated and actual SPP values to converge. Once both friction factors are calculated, the model is used effectively for control. From this initial calibration, the friction factors are continuously adjusted by the estimator, but such adjustments are minor, as seen in Figure 2.6 and Figure 2.7, which present normal drilling scenarios. Model calibration is useful for both full-closed loop and semi-closed loop control configurations. A full-closed loop control calibration essentially occurs at every time step when the estimator algorithm is run. In the semi-closed loop configuration, however, calibration is performed as often as bottomhole data becomes available. As data is received on the surface it is used to recalibrate the simplified model as required.

المنارة للاستشارات
www.manaraa.com

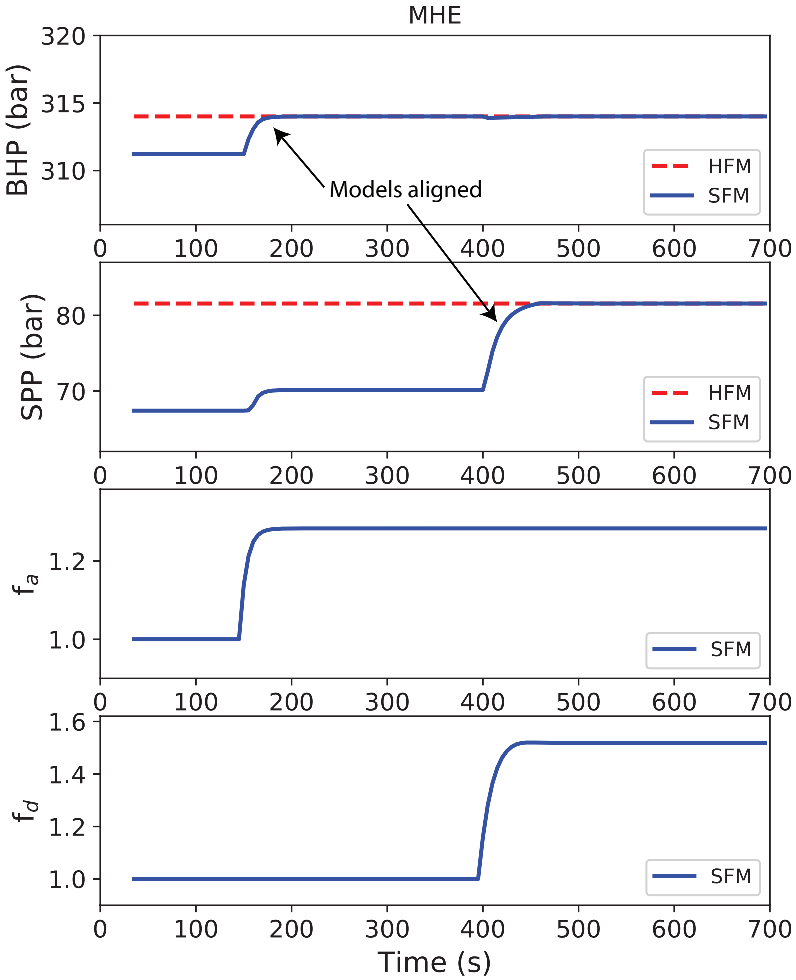

Figure 2.5: Model calibration using MHE

### 2.6.2 Normal Drilling

Figure 2.6 and Figure 2.7 display the results of normal drilling case study for the semi-closed loop and full-closed loop configurations, respectively. In the semi-closed loop case the BHP is controlled by using the standpipe pressure in the objective function of the controller. It is assumed that mud pulsing is used to communicate bottom hole conditions to the surface. This is compared to the full-closed loop conditions where WDP is assumed and BHP measurements are regular and frequent. As explained with Figure 1.6, the model is first calibrated. This calibration

www.manaraa.com

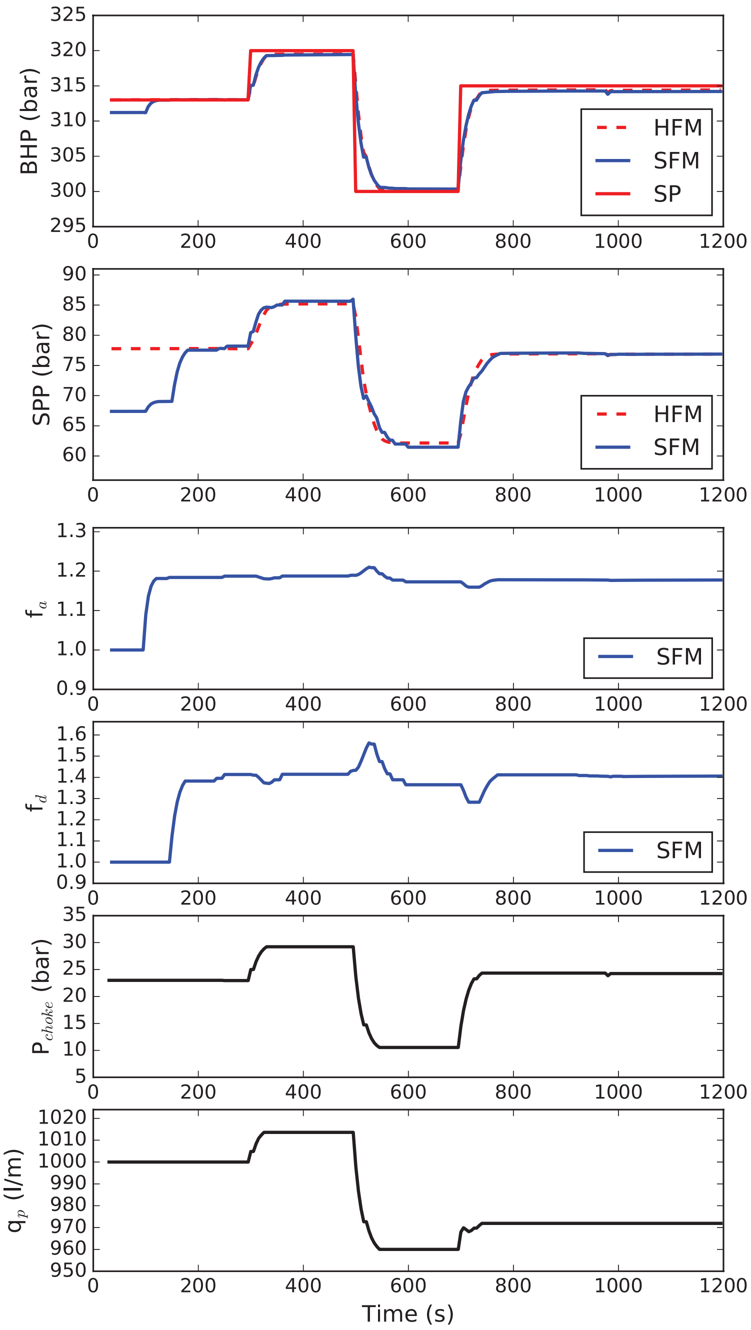

Figure 2.6: Control performance for normal drilling scenario - Semi-closed loop

of the friction factors is observed in Figure 2.6 and Figure 2.7 between 0 and 200 seconds. The BHP control is more effective in a full-closed loop scenario as the controller is able to use actual bottomhole conditions to inform the control moves. However, it is of interest that the improvement in control performance observed in the full-closed loop case is minor and that the full-closed loop

المنارة للاستشارات
www.manaraa.com

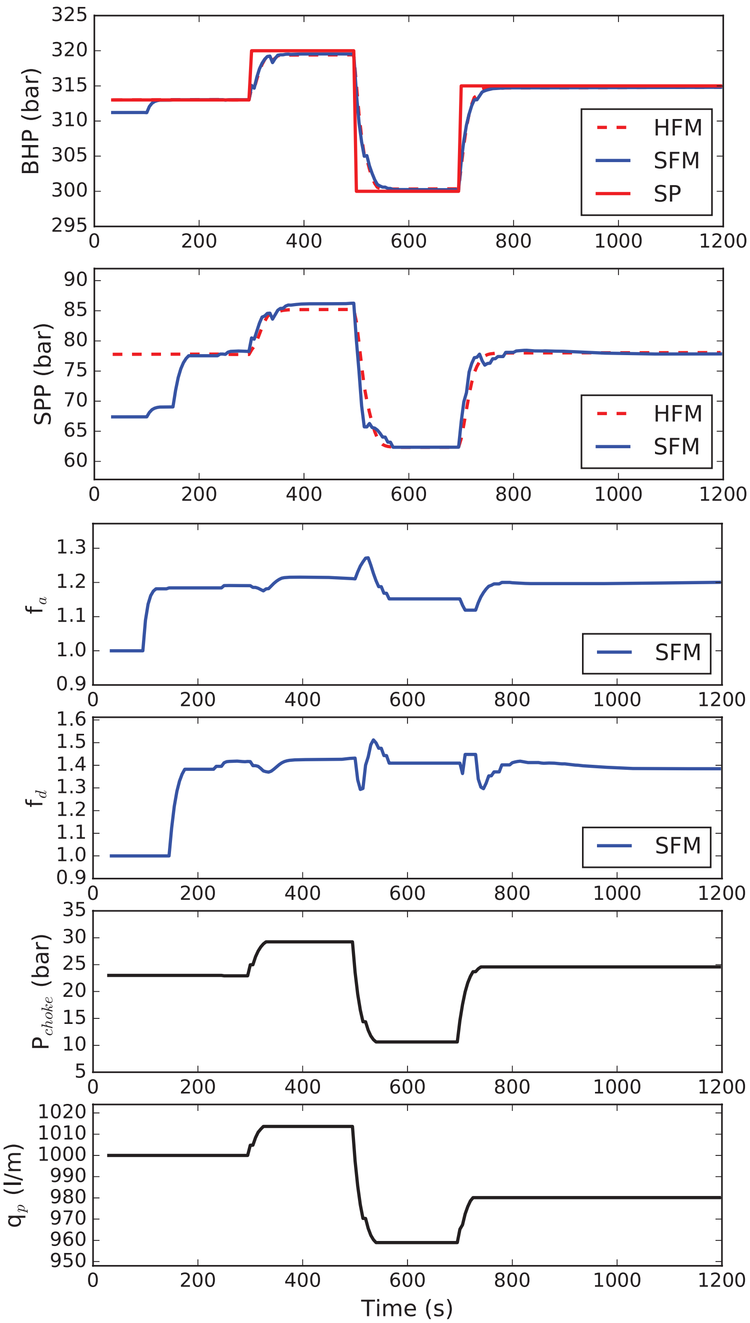

Figure 2.7: Control performance for normal drilling scenario - Full-closed loop

scenario brought the BHP about 0.5 bar closer to the setpoint as compared to the semi-closed loop scenario. While this is not an exhaustive survey across a multitude of well conditions, it is indicative of the effectiveness of using a semi-closed loop system that employs a SFM.

www.manaraa.com

The differences in a semi-closed loop system and a full-closed loop system are a result of the data the estimator uses to determine the annulus and drill string friction factors. As is previously addressed, the semi-closed loop system relies on standpipe pressure, and the objective function adjusts the friction factors to achieve convergence of the standpipe pressures of the SFM and HFM. This convergence is observed in the standpipe results of Figure 2.6. There is a slight offset observed in the BHP of Figure 2.6 due to the use of the standpipe pressure in the estimator objective function. The opposite effect is seen in the full-closed loop scenario presented in Figure 2.7. The BHP is maintained closer to the set point because the estimator is using the BHP data in its objective function. The SPP is observed to diverge more significantly in the full-closed loop case because the estimator is no longer relying primarily on the standpipe pressure to estimate the friction factors. The variations in friction factors between the two cases can be observed in Figure 2.6 and 2.7. They are similar for the most part, but the dynamic portions vary significantly and as the friction factors steady out between 900 and 1200 seconds the full-closed loop scheme estimates an annulus friction factor slightly higher than that of the semi-closed loop and a drill string friction factor slightly lower than that of the semi-closed loop scenario. Ultimately, the differences between the two scenarios are minimal and demonstrate the effectiveness of the estimator and controller using a SFM in both full and semi-closed loop control schemes. Ultimately very similar control moves were made (as seen in Figs. Figure 2.6 and 2.7), and the resulting BHP measurements differed by less than one bar.

### 2.6.3 Pipe Connection

The pipe connection procedure results are shown in Figure 2.8 and 2.9. During the pipe connection procedure, mud flowrate moves through a wider operational range from the range of normal drilling to the zero flowrate which produces greater model mismatch than the normal drilling scenario. According to the settings and models of this study, the primary factor of the model mismatch is the mud flowrate because the friction factor of the drill string and annulus is only important when the mud is flowing. At the beginning of the case study, the model calibration proceeds until the MPC control starts at 400 seconds. From 600 seconds, mud flowrate starts ramping down and stays at the zero flowrate for about 300 seconds until the new segment of a drill string is added. The mud flow rate is then ramped back up to the normal drilling range (1000

www.manaraa.com

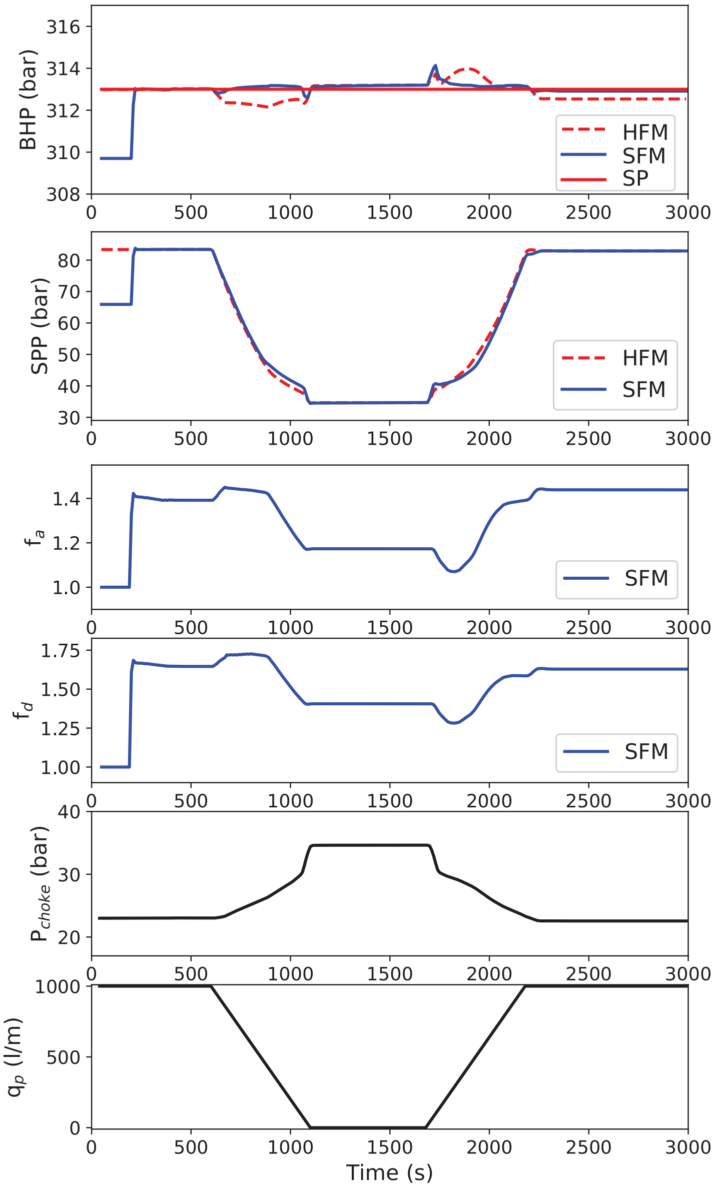

Figure 2.8: Control performance for pipe connection scenario - Semi-closed loop

$l/min$). As the mud flow ramps down, the BHP is maintained by compensatory moves in the choke pressure. Because it is a planned change in the mud flow, the ramp down is communicated to the predictive controller and the controller designs effective moves to maintain a steady bit pressure through the pipe connection procedure. MHE continuously adjusts the annulus and drill string friction factor to match the BHP or SPP, depending on the control mode. Figure 2.8 and 2.9 show the results of the semi-closed loop and full-closed loop control mode respectively. Although the

المنارة للاستشارات
www.manaraa.com

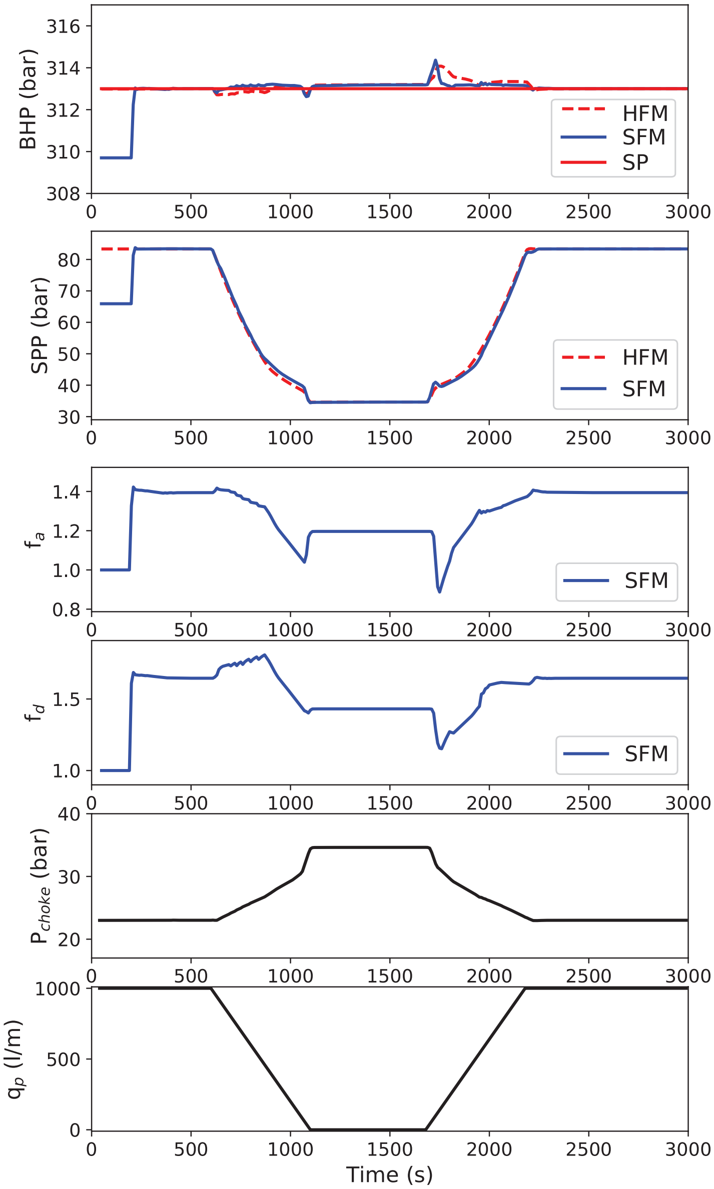

Figure 2.9: Control performance for pipe connection scenario - Full-closed loop

mud flowrate is varied greatly, both control modes show acceptable control performance maintaining the BHP within ± 1 bar deviation. However, the semi-closed loop mode shows slightly worse control performance than the full-closed loop mode after mud flowrate ramps up completely because the annulus friction factor ($f_a$) stops adjusting at 2300 seconds It continuously adjusts only in full-closed loop mode. The objective of MHE to minimize model and process discrepancies is

المنارة للاستشارات
www.manaraa.com

satisfied for the semi-closed loop mode at 2300 seconds by eliminating the SPP difference between the HFM and SFM. However, the BHP difference still exists.

### 2.6.4 Mud Density Displacement

The results in Figure 2.10 and 2.11 demonstrate the impact of changes in drilling fluid density on the estimated friction factor and the resultant changes in the choke pressure and drilling fluid flow. The differences between a semi-closed and full-closed loop mud density displacement scenario are also displayed. The drilling fluid density change is observed at 0.5 hours as the density is stepped up from 1.5 S.G. to 1.6 S.G. The choke valve is subsequently ramped down over a 2.5 hour period between 0.5 and 3 hours. It is observed that because of the aforementioned system changes the drilling fluid flow slowly decreases to further counteract the increase in density. This indicates that shutting down the choke valve does not provide enough pressure relief and the controller selectively relies on the drilling fluid flow to maintain control. Additionally, the standpipe pressure drops off substantially but the BHP stays high as a result of the higher density drilling fluid. In the full-closed loop configuration, the simplified model matches the simulated real world conditions more closely, which has the result of maintaining the quality of BHP control provided by the MPC controller.

## 2.7 Conclusions

This study investigates the BHP control performance of an MPC controller that uses a simplified, physics-based flow model. Full-closed and semi-closed loop control schemes are presented and in each scheme the BHP is shown to be successfully controlled in conditions of normal drilling, pipe connection, and mud density displacement. The results demonstrate tight controller performance that successfully maintains the BHP to within one bar of the set point in each scenario. Additionally, MHE calibrates the model and effectively estimates the drill string and annulus friction factors. The effectiveness of the controller is predicated on the quality of the estimator, and the present study demonstrates that tight BHP control is achieved in conjunction with estimation of the unknown model parameters, $fa$ and $fd$.

المنارة للاستشارات
www.manaraa.com

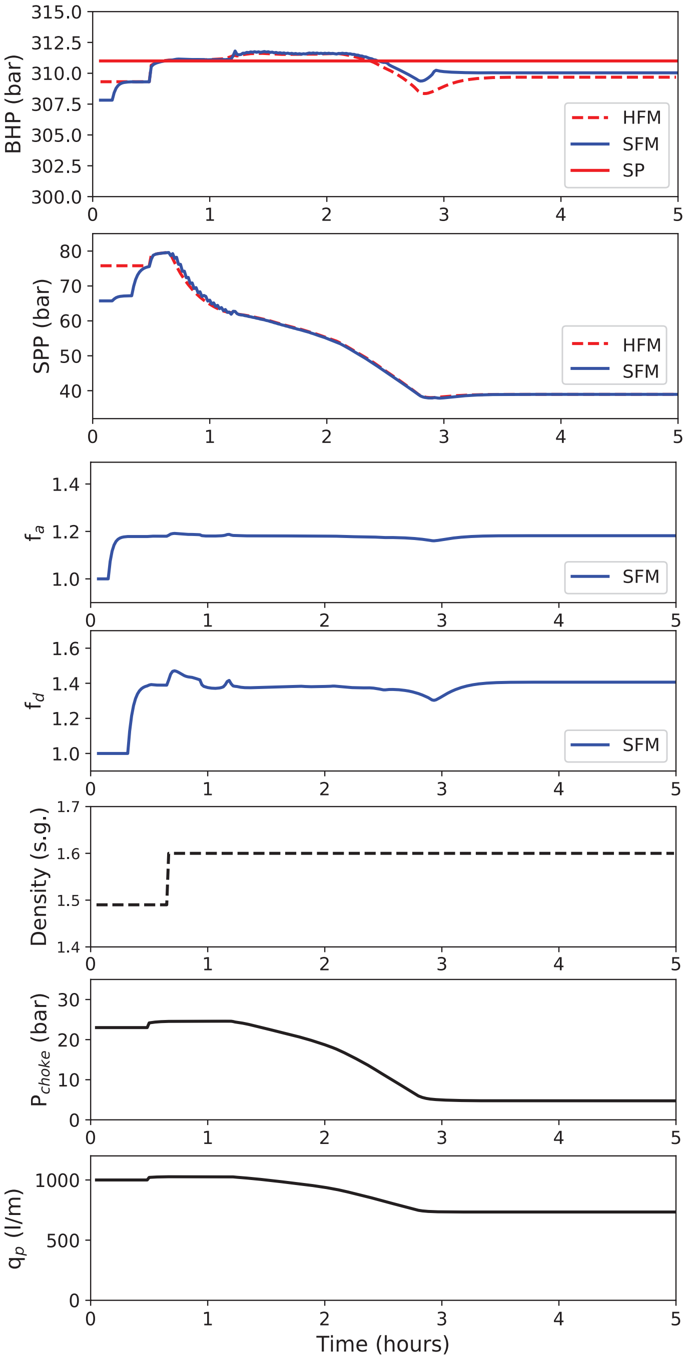

Figure 2.10: Control performance for density displacement scenario - Semi-closed loop

In normal drilling scenarios, the BHP is controlled and regulated to a desired setpoint. Control is improved with a full-closed control scheme, but the advantages over a semi-closed loop are marginal. Similarly, when controlling BHP during pipe connection it is more effective to

www.manaraa.com

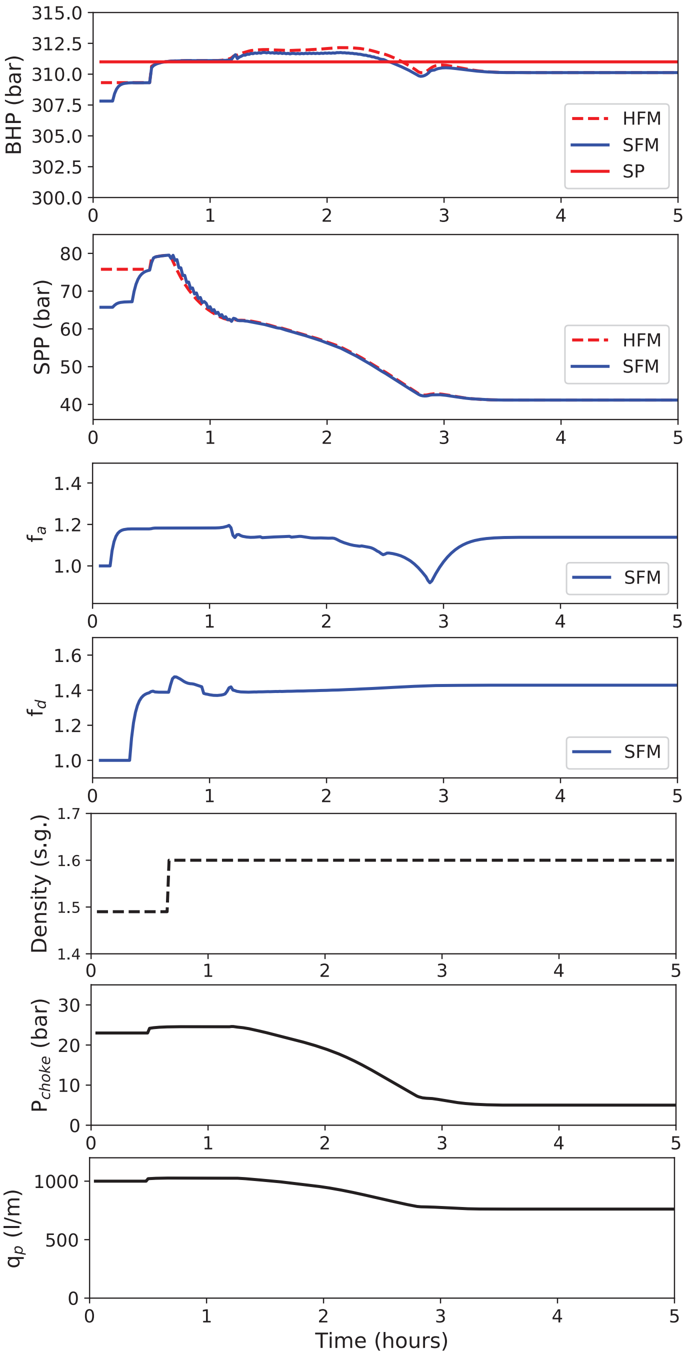

Figure 2.11: Control performance for density displacement scenario - Full-closed loop

use a full-closed loop, but semi-closed loop is also a viable option with feedforward information. Inclusion of feed forward control in the MPC algorithm enables effective BHP control in this scenario. Model mismatch is introduced by pipe connections because of loss of measurements, and model recalibration should be performed after such a procedure. In mud density displacement the

المنارة للاستشارات
www.manaraa.com

semi-closed loop again developed some mismatch that is best remedied by a model recalibration, but mismatch is minimal and the recalibration is not critical immediately following a period of mud density displacement. The full-closed scheme again proves more effective than the semi-closed scheme for mud density displacement.

The MPC controller handles the several scenarios successfully and the results indicate that a simplified model can be used to achieve BHP control. Such a model would be effective on most oil rigs currently in operation as the data shows that the differences between full-closed loop and semi-closed control schemes is minimal. The results of this study solidify the need of a SFM in MPD. A SFM can be a useful tool for controlling systems using mud pulsing or WDP, and such control comes at a smaller computational cost than use of a HFM and offers the benefit of tight control that improves drilling quality as well as the opportunity to drill more complex wells that have narrow pressure requirements.

المنارة للاستشارات
www.manaraa.com

# CHAPTER 3. BOTTOM HOLE PRESSURE REGULATION USING HAMMERSTEIN-WIENER NONLINEAR MODEL PREDICTIVE CONTROL FOR MANAGED PRESSURE DRILLING

## 3.1 Introduction

The recent downturn of the crude oil market motivates improvements in cost effective oil and gas well manufacturing and production. Automation is one possible solution to minimize costs and well completion time. Automation systems can improve safety and convenience and enable optimization strategies. The oil well drilling industry is transitioning to automation systems as downhole sensors, communication, and control technology improves. Thanks to modern telemetry and integration of control systems in new drilling rig designs, several opportunities are opened for Managed Pressure Drilling (MPD) automation and optimization strategies. One of these technologies is Model Predictive Control (MPC). MPC has successfully been applied in many industries [24]. MPC vendors report that over 4,600 MPC applications were in use by the early 2000s with most applications in the downstream industry. Several features make the technology attractive to the drilling industry. First, MPC has a prediction feature that employs a process model, either determined from data or from physics-based simulators. This feature predicts future constraint violations and anticipates behavior of the process in advance. Processes that have long time constants and time delay or inverse response can be effectively managed. Second, MPC deals with multiple variables at a time, considering the coupling effect between variables. It is able to control multi-input and multi-output (MIMO) systems with single-input and single-output control (SISO) systems are typically implemented with less advanced methods such as Proportional, Integral, and Derivative (PID) control. Third, MPC accommodates nonlinear processes by using Nonlinear Programming Solvers (NLP) and efficient methods to discretize the control and prediction horizon. Fourth, MPC has a range feature that specifies an acceptable control range instead of always driving to a desired target set point. This gives more freedom to operate within an upper and lower

المنارة للاستشارات
www.manaraa.com

range or to drive to a limit, especially when the system has more than one controlled variable (CV). The range control feature can reduce conflicted situations when set points for individual CVs are simultaneously unachievable. Fifth, MPC allows optimization strategies to push the operation to a more beneficial point, while keeping within an acceptable range. All of these advantages are compared to the well-known PID controller that has the advantage of simple implementation and tuning.

There are the several characteristics of MPD that are improved with MPC technology. First, it is critical to regulate the BHP within a pressure window during MPD operations. Low pressures lead to unexpected gas influx (kick) and high pressures lead to formation damage or lost drilling fluid (mud) circulation. Lower pressure has the effect of increasing ROP because it reduces the chip hold-down effect [40]. Related studies demonstrate this benefit by using simplified pressure hydraulics and an ROP model [20, 21]. The set range control and optimization functionality of MPC are important for these multivariate operation criteria. Second, in comparison to conventional drilling operation, MPD has more manipulated variables (MVs) such as choke valve, main mud pump and backpressure pump that move in coordination to maintain a BHP. All three MVs are adjusted simultaneously by exploiting the multivariate capabilities of MPC. Lastly, the inherent nonlinear and saccadic nature of drilling is a challenge for the application of automation. Figure 3.1 shows the nonlinearity of the drilling operation between the main variables. The simulated data is obtained from a detailed physics-based drilling simulator, WeMod. A full nonlinear model can be applied to control MPD automation but there are different types of nonlinear models that have been demonstrated. Many previous research studies in drilling automation have established reduced order models by capturing the main dynamics of the drilling process [28, 32, 33, 37]. Although using simplified low order models reduces the computational time significantly, solving the numerical optimization problem in the MPC algorithm with nonlinear equations is still computationally demanding for real-time control purposes. Moreover, those models use several variables that are not measured and must be estimated. This estimation step adds an additional layer of complexity and computational burden. In contrast with a first principles model, an empirical step response model such as those used in linear Model Predictive Control (LMPC) are widely used in many industries. However, these linear models are not sufficient to capture the nonlinear nature of drilling. Hammerstein-Wiener models are the most widely implemented method of empirical nonlinear

المنارة للاستشارات
www.manaraa.com

models in industry [48–53]. There are rich sources of the Hammerstein-Wiener model identification research [54–56]. The Hammerstein-Wiener models employ input and output static nonlinear blocks before and after the linear dynamic blocks. Because the nonlinear portions of the model are not included in the MPC calculation, the computational burden is significantly reduced. This model structure assumes that the time constant of the process does not vary significantly while the static gain varies greater at different operation points. Thus, this type of nonlinear model performs better for the processes that have a relatively short time constant value and smaller time constant variation throughout the extended operation range. For the processes that have an extensive time constant variation or for the combined control and scheduling system, the time constant variation should be managed by the model structure to maintain the consistent control performance [57]. This study demonstrates a Hammerstein-Wiener based NMPC for BHP regulation in drilling. The control performance of the Hammerstein-Wiener based NMPC is compared to the ubiquitous PID controller in various scenarios that frequently occur in drilling operations, such as a pipe connection procedure and with unexpected gas influx.

## 3.2 Hammerstein-Wiener Based Model Predictive Control

The structure of Hammerstein-Wiener NMPC for drilling is detailed in this section. The Hammerstein-Wiener model is an extended form of LMPC. It uses the same algorithm as LMPC to optimize the linear dynamic portion of the model. As such, Hammerstein-Wiener NMPC captures the input and output nonlinearities with the computational robustness and simplicity of LMPC. To add the nonlinear control elements to LMPC, the Hammerstein-Wiener model employs static nonlinearity blocks that process the input and output values of the linear dynamic model block. The static nonlinearity blocks are static functions that are separated from the quadratic programming (QP) optimization problems in the MPC algorithm [58, 59]. Therefore, it allows a gain-scheduling concept for a nonlinear process without significantly increasing the computational complexity. As shown in Figure 3.2, the linear dynamic model (**G**) is located in between the input and output static nonlinearity blocks (**F** and **H**).

Various types of models can be used for the linear dynamic model. In this study, a state space model is chosen over other types such as a Finite Impulse Response (FIR) model. Eqn. (3.1)

المنارة للاستشارات
www.manaraa.com

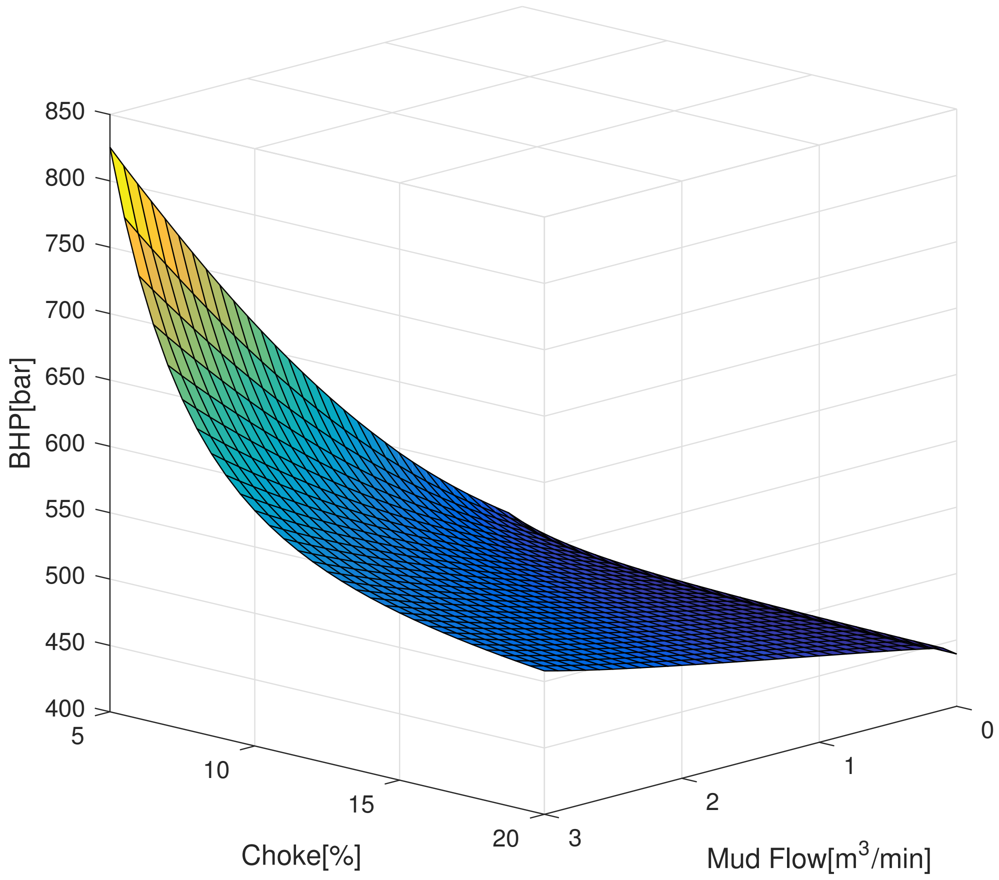

Figure 3.1: Nonlinearity analysis of drilling operation

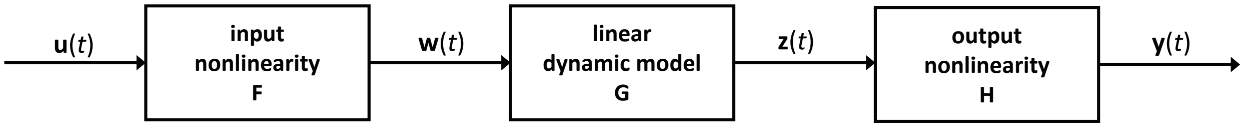

Figure 3.2: Structure of the Hammerstein-Weiner Model

and Eqn. (3.4) represent the input and output nonlinearity blocks (**F**, **H**) respectively and both Eqn. (3.2) and (3.3) describe the state space form of the linear dynamic model (**G**):

www.manaraa.com

$$\mathbf{w}(t) = \mathbf{F}(\mathbf{u}(t)) \tag{3.1}$$

$$\frac{dx(t)}{dt} = \mathbf{A}\mathbf{x}(t) + \mathbf{B}\mathbf{w}(t) \tag{3.2}$$

$$\mathbf{z}(t) = \mathbf{C}\mathbf{x}(t) \tag{3.3}$$

$$\mathbf{y}(t) = \mathbf{H}(\mathbf{z}(t)) \tag{3.4}$$

where, the vector $\mathbf{u}(t) \in \mathbf{R}^m$ and $\mathbf{w}(t) \in \mathbf{R}^m$ are the input variables of the input nonlinearity block and linear dynamic model block, respectively. The input value, $\mathbf{u}(t)$, is the actual input value from the process and is converted to an internal variable $\mathbf{w}(t)$ by the input nonlinearity function $\mathbf{F}$. The vector $\mathbf{x}(t) \in \mathbf{R}^n$ represents the state variable of the state space model. The vectors $\mathbf{z}(t) \in \mathbf{R}^l$ and $\mathbf{y}(t) \in \mathbf{R}^l$ are the output variables of the linear dynamic model and output nonlinearity block, respectively. Similar to $\mathbf{u}$ and $\mathbf{w}$, internal variable $\mathbf{z}(t)$ is converted to an actual prediction variable $\mathbf{y}(t)$ through the output nonlinearity block $\mathbf{H}$. $\mathbf{A}$, $\mathbf{B}$ and $\mathbf{C}$ denote the state, input, and output matrix of the state space model. The function $\mathbf{F}$ and $\mathbf{H}$ in the nonlinearity blocks could be a nonlinear relationship such as polynomial, power series, or piecewise linear function. In this study, we use the piecewise linear function for nonlinearity blocks discussed in the case study section.

The Hammerstein-Wiener model is utilized in the MPC platform in two main steps: ‘Prediction’ and ‘Optimization’. In the prediction step, a sequence of future moves of the CVs is predicted by processing the set of past movements of the MVs through the process dynamics model. Then, in the optimization step, a sequence of optimized future MVs movements is calculated by solving a QP optimization problem. The QP objective function is designed to minimize the difference between the predicted value and desired trajectory of the CVs. The first MV move of the sequence is implemented to modify the choke position and pump rates. The entire procedure is repeated for every sampling time. The additional steps for the Hammerstein-Wiener model are the processing of input and output values for the LMPC. This involves reverse processing the actual CV targets or ranges through the inverse nonlinearity block before it goes into the MPC block. Additionally, the internal MV output which is reverse transformed and applied to the process. Note that the nonlinearity blocks are inverted for the control schematic. The structure of the Hammerstein-Wiener based MPC system is shown in Figure 3.3.

للاستشارات المنارة
www.manaraa.com

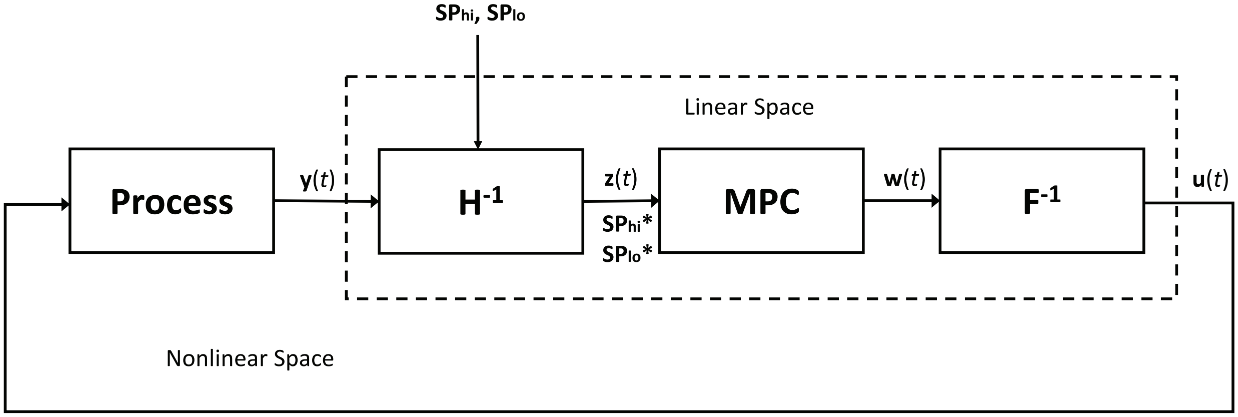

Figure 3.3: Structure of the Hammerstein-Weiner based MPC system

Mathematical expressions of the Hammerstein-Wiener MPC are shown below. The upper and lower bound of control input ($sp_{hi}$, $sp_{lo}$) and control input itself ($y$) are transformed by inverse output nonlinearity function $h^{-1}$ shown in Eqn. (3.5), and (3.6). The control output ($w$) is transformed by inverse input nonlinearity function $f^{-1}$ shown in Eqn. (3.7).

$$sp^*_{hi}(t) = h^{-1}(sp_{hi}(t)) \quad \text{and} \quad sp^*_{lo}(t) = h^{-1}(sp_{lo}(t)) \tag{3.5}$$

$$z(t) = h^{-1}(y(t)) \tag{3.6}$$

$$u(t) = f^{-1}(w(t)) \tag{3.7}$$

The QP objective function used in this study is the $\ell_1$-norm type objective which has many advantages especially for the multiple objective optimization [39]. The $\ell_1$-norm objective function with the parameters associated with Hammerstein-Wiener structure is shown in Eqns (3.8) - (3.15) and Table 3.1.

المنارة للاستشارات
www.manaraa.com

$$\underset{z,w}{min}\Phi = Q_{hi}^{T}(e_{hi}) + Qlo^{T}(e_{lo}) + (z_m)^{T}c_z + (w)^{T}c_w + (\Delta w)^{T}c_{\Delta w} \tag{3.8}$$

$$s.t. \;\; 0 = f(\dot{x}, x, u, d) \tag{3.9}$$

$$0 = g(y_x, x, u, d) \tag{3.10}$$

$$a \geq h(x, u, d) \geq b \tag{3.11}$$

$$\tau_c \frac{\Delta y_{t,hi}}{\Delta t} + y_{t,hi} = sp_{hi} \tag{3.12}$$

$$\tau_c \frac{\Delta y_{t,lo}}{\Delta t} + y_{t,lo} = sp_{lo} \tag{3.13}$$

$$e_{hi} \geq (y_m - y_{t,hi}) \tag{3.14}$$

$$e_{lo} \geq (y_{t,lo} - y_m) \tag{3.15}$$

Table 3.1: Summary of parameters used in $\ell_1$-norm objective function for H-W MPC

| **Parameter** | **Description** |
|---|---|
| $sp_{hi}$, $sp_{lo}$, $sp_{hi}*$, $sp_{lo}*$ | Actual and transformed (*) value of upper and lower bound |
| $h^{-1}$, $f^{-1}$ | Inverse nonlinearity block function |
| $\phi$ | Objective function |
| $z_m$ | Model output values $(z_{m,0},\ldots,z_{m,n})^T$ or predicted output values |
| $w$ | Inputs |
| $x$ | States |
| $z_{t,hi}, z_{t,lo}$ | Desired trajectory dead-band |
| $Q_{hi}, Q_{lo}$ | Penalty outside trajectory dead-band or weighting factor |
| $c_z, c_w, c_{\Delta w}$ | Cost of $z$, $w$, and $\Delta w$, respectively |
| $i$ | Equation residuals |
| $j$ | Output function |
| $k$ | Inequality constraints |
| $\tau_c$ | Time constant of desired controlled variable response |
| $e_{lo}$ | Slack variable below the trajectory dead-band |
| $e_{hi}$ | Slack variable above the trajectory dead-band |

المنارة للاستشارات
www.manaraa.com

## 3.3 Case Study

In this section, the wellbore condition and scenarios are described. It simulates a vertical geometry well with the MPD rig. The MPD rig has a choke valve, a main mud pump, and a back pressure pump as maneuvers for the BHP regulation. The detailed parameters of the wellbore condition are referred from the other study [60] and shown in Table 3.2. For the BHP measurement, WDP is used for all scenarios. Unlike the traditional mud-pulse telemetry, WDP increases the data transmission rate up to $10^4$ - $10^5$ bits per second and provides reliable bottomhole data to the surface to enable MPD control systems in real-time [41].

Table 3.2: Wellbore Conditions II

| **Parameter** | **Value(AES)** | **Value(SI)** |
|---|---|---|
| Well depth | 11,800 ft | 3,600 m |
| Riser inner diameter | 19” | 0.48 m |
| Water depth | 590 ft | 180 m |
| Casing inner diameter | 9” | 0.23 m |
| Casing depth | 7,100 ft | 2,164 m |
| Drill string average outer diameter | 4.5” | 0.12 m |
| BHA length | 150 ft | 45.7 m |
| BHA average outer diameter | 6.7” | 0.17 m |
| Open hole/bit size | 8.5” | 0.2 m |
| Reservoir depth | 9840 ft | 3,000 m |
| Reservoir Pore Pressure | 401.0 bar/1.364 s.g. | 401.0e+05 Pa/1.364 s.g. |
| Initial mud density | 1.24 s.g. | 1.24 s.g. |

An important factor in the MPC design is the relationship between inputs and outputs. Figure 3.4 shows the MPC design matrix with +/- signs that denote the positive or negative gain relationships. Various process dynamics models could be used for these relationships such as transfer function or state space forms that have equivalent relationships. These types of models represent both transient behavior and steady state gain. In Figure 3.4, BHP ($p_{bit}$) is the main controlled variable (CV) for the normal operation and pipe connection procedure. The Mud flow balance ($q_{bal}$) is considered as an additional CV for kick attenuation. The three MPD manipulated variables are choke opening ($z_{choke}$), back pressure pump ($q_{back}$), and main mud pump ($q_p$). All three variables play a role as MVs except for the pipe connection procedure where the main mud

المنارة للاستشارات
www.manaraa.com

flow is manually ramped up and down. Therefore, the main mud flow is considered as a ramped input for the pipe connection procedure. The MPC algorithm reflects the influence of the ramping sequence on the control calculation so that it compensates for the loss or gain of mud flow before it drives the BHP away from a target value.

| | | MV/DV | | |
|---|---|---|---|---|
| | | $Z_{choke}$ | $q_{back}$ | $q_p$ |
| CV | $p_{bit}$ | - | + | + |
| | $q_{bal}$ | - | + | + |

Figure 3.4: Model matrix with the positive and negative interaction between CVs and MVs/DVs

### 3.3.1 Normal Drilling

Maintaining the wellbore pressure within a pressure window is one of the highest priorities for normal drilling. Within this pressure window, it is best to maintain pressure near the lower limit of pore pressure for maximum ROP. This is not only to reduce mud loss in certain zones, but also because the pressure difference between wellbore and reservoir generate the chip hold-down effect that causes lower ROP [40]. Although lower pressure is desired, approaching the reservoir pore pressure increases the possibility of a gas influx. In the normal drilling scenario, two aspects of NMPC are tested. The first is control performance when the set point or set range is changed, called servo control. The set range of the BHP is changed to sufficiently cover a wide operation range. All three MVs (choke opening, main mud pump flow, and back pressure pump) are actively adjusted to meet the new set range of BHP. The weighting factors in the objective function for each MV are tuned to adjust the relative movements among the MVs. The second aspect is related to an optimization feature of MPC. While the BHP is maintained in the desired set range, the linear programing (LP) objectives for the CVs and MVs drive the variables to the upper or lower limit of each. The parameters $c_z$ and $c_w$ in Eq 3.8 are the cost parameters for the minimized LP objectives. They are positive constants to push the BHP to the low value of the range near the pore pressure.

www.manaraa.com

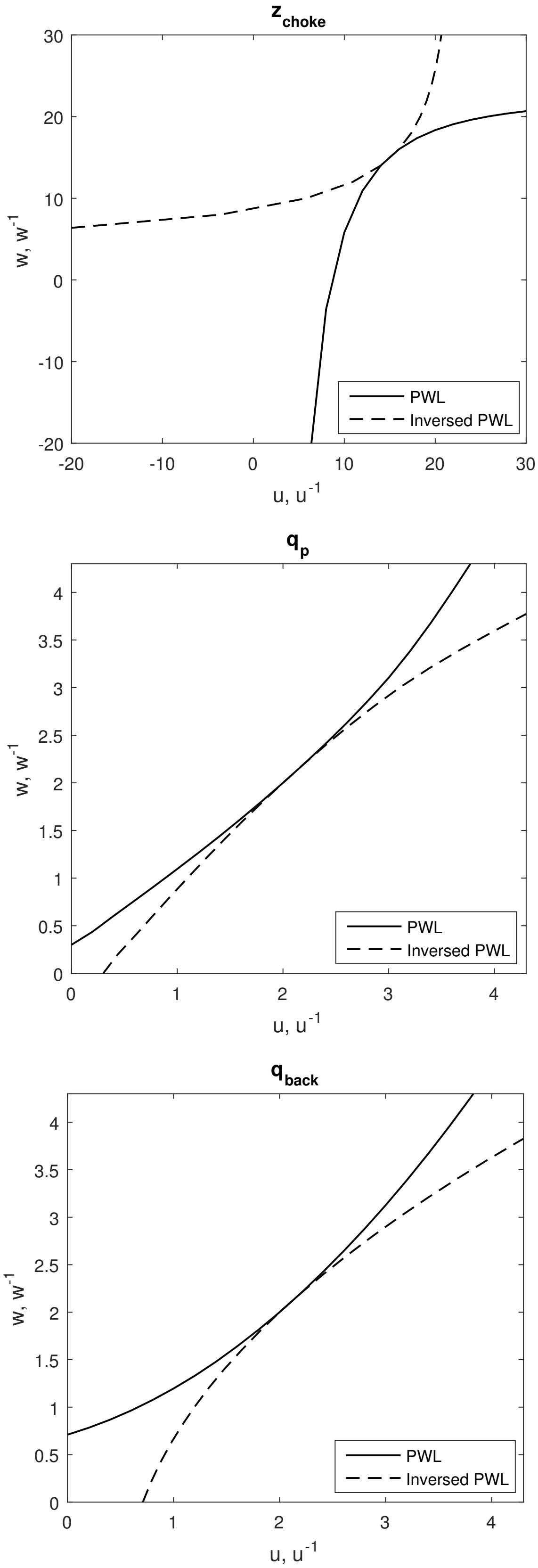

Figure 3.5: Piecewise linear function for input nonlinearity blocks

www.manaraa.com

### 3.3.2 Pipe Connection

Pipe connection is the addition of multiple sections of drilling pipe to the existing drill string as the drill bit penetrates the formation. Based on a rough calculation with typical ROP and length of a single pipe stand, the pipe connection procedure takes place every one to three hours [46]. During the procedure, the main mud pump flowrate is ramped down to zero and waits until a new pipe is added and then ramped back up to normal drilling operation. The BHP is formed by three different sources, hydrostatic pressure of mud and cuttings, annulus friction pressure loss by mud flow rate, and back-pressure exerted by the back-pressure pump and choke valve. By ramping down the main mud flow rate, one of the pressure sources exerted on the bottomhole is lost. The back-pressure system includes the choke valve and back-pressure pump and is adjusted to compensate for the BHP decrement. Note that the hydrostatic pressure does not change during the entire pipe connection procedure. In the MPC configuration for pipe connection procedure, the main mud pump flowrate ($q_p$) switches from an optimized degree of freedom to a fixed ramp input. The predefined ramping sequence of the mud flowrate ($q_p$) is not a part of the MPC output. However, it has a significant effect on the BHP and is therefore considered by MPC calculation. By having this feedforward input in the MPC, the pressure control performance is significantly improved in comparison with the case that fully relies on feedback control.

### 3.3.3 Kick Attenuation

When the drill bit enters a formation that has high reservoir pressure, formation gas may unexpectedly penetrate into the wellbore as the pore pressure exceeds the BHP. The gas influx from the formation may require more aggressive well control methods or may cause loss of well control in extreme circumstances. To prevent such problems, any detected gas influx above a certain threshold required for well control is typically circulated out after the well is shut in. In MPD, the mud pump flowrate and choke valve regulate the BHP without shutting in the well and stopping the drilling process. The kick is conventionally detected by monitoring the mud pit levels or by observing an imbalance between mud pump flow and returning mud. Other kick detection methods include monitoring of unexpected increase in annulus pressure as the dissolved gas escapes the formation or an unexpected decrease in hydrostatic pressure due to the expansion

المنارة للاستشارات
www.manaraa.com

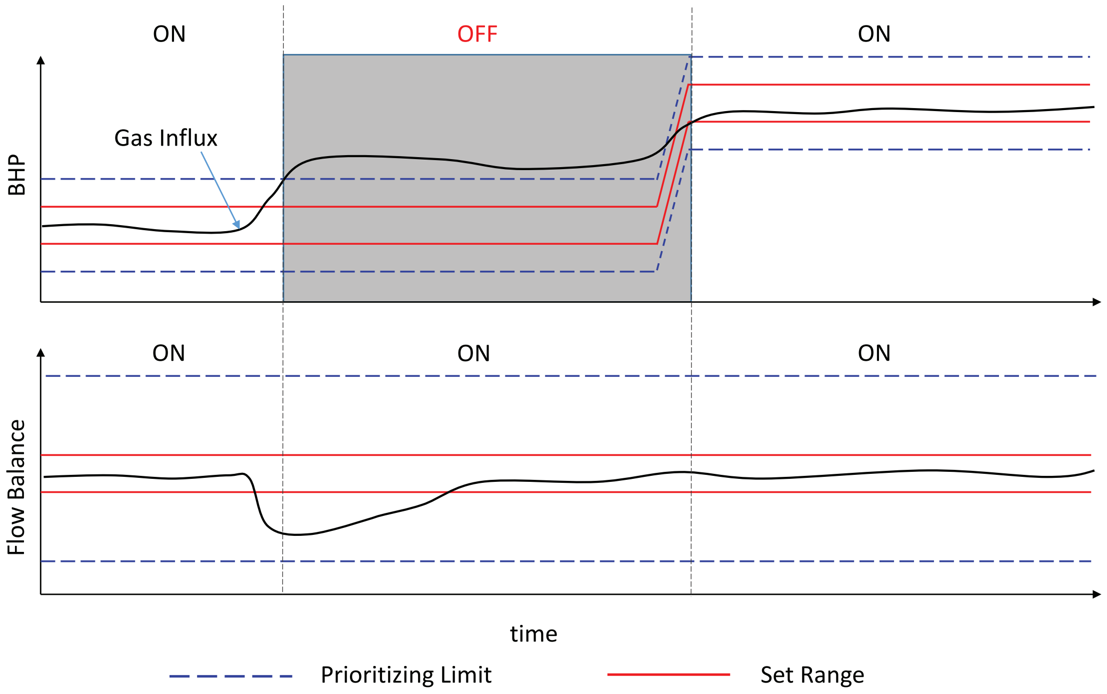

Figure 3.6: Illustration of prioritizing function for kick attenuation

of the dissolved gas as it travels with the mud back to the surface. The control strategy for the BHP should be differentiated between the normal operation and the kick situation. To decrease the high BHP in normal operation, the choke valve opens and the mud pump flowrate decreases. During a kick, the same control actions, however, still allow or even accelerate the gas influx to rise up to the surface through the mud circulation. The strategy in the previous research [21] correctly decreases the choke valve opening and increases the mud pump flowrate by switching the CV from BHP ($p_{bit}$) to choke valve pressure ($p_c$) with a calculated higher set point. The other research proposed a different switching method between BHP control and mass balance control with a PID control algorithm [30]. In this study, the mass balance control concept is adopted with an MPC algorithm. The flow balance is added to the BHP control configuration as a second CV without additional switching logic. However, by introducing the second CV, conflicts potentially arise from physically infeasible constraints of all the CVs and MVs. These situations are significantly reduced by the aforementioned MPC advantages, such as the range control feature and weight factors for the CVs in the objective function to prioritize conflicting objectives. In addition to these, a CV prioritization is added to exclude a CV from the MPC calculation in a specific condition. The

www.manaraa.com

condition is defined by adding additional high and low limits for CVs that are normally higher and lower than set ranges. When the current value of one CV violates these limits, the controller temporarily gives up controlling this CV while still controlling the other CVs that stay within in the specified limits. A simplified illustration in Figure 3.6 shows how this method works in the kick situation. When BHP increases beyond the prioritizing limit, MPC immediately turns off the BHP CV and fully focuses on the Flow Balance CV. After mitigating the gas influx, the new set range is set based on the stabilized BHP plus a safety margin. Then, the controller automatically turns on the BHP CV again by having a current value within the prioritizing limit.

## 3.4 Results and Discussions

The simulation results of the three previously described scenarios are detailed in this section. Figure 3.7 and 3.8 show the result of normal drilling operation. The servo control performance is tested for both PID and NMPC. The SISO configuration of PID allows the controller to move one MV at a time. The choke valve opening ($z_c$) is a single MV for the PID controller while NMPC adjusts choke valve opening ($z_c$) and mud pump flowrate ($q_p$) simultaneously. In order to test the performance for a severe situation, greater changes in the set point than typical operation are demonstrated. The PID controller cannot reach the set point changes, even though the choke valve moves are more aggressive and cover the full range of the valve opening (0 - 100%). This result shows that the operation is limited into a narrow pressure range with adjustments only to the choke valve opening. Improved performance is demonstrated by using the mud pump flowrate to add or remove the pump head pressure in the wellbore pressure. In the NMPC result, BHP quickly follows the set point changes by coordinating adjustments to the two MVs.

Figure 3.9 and 3.10 show the results of the pipe connection procedure. Unlike the normal drilling scenario, the pipe connection procedure covers a wider operation range by ramping down and up the main mud pump from the normal operation range to zero and back again. In this case, the nonlinearity problems are more evident than in a normal drilling operation. Similar to the normal operation case, the PID controller fails to maintain the BHP within an acceptable range (Figure 3.9). Although it fully closes the choke opening while ramping down the mud pump flowrate, it is not sufficient to compensate for the mud pump head pressure loss. For this specific case, MPD employs the back pressure pump to exert additional pressure by maintaining the mud

المنارة للاستشارات
www.manaraa.com

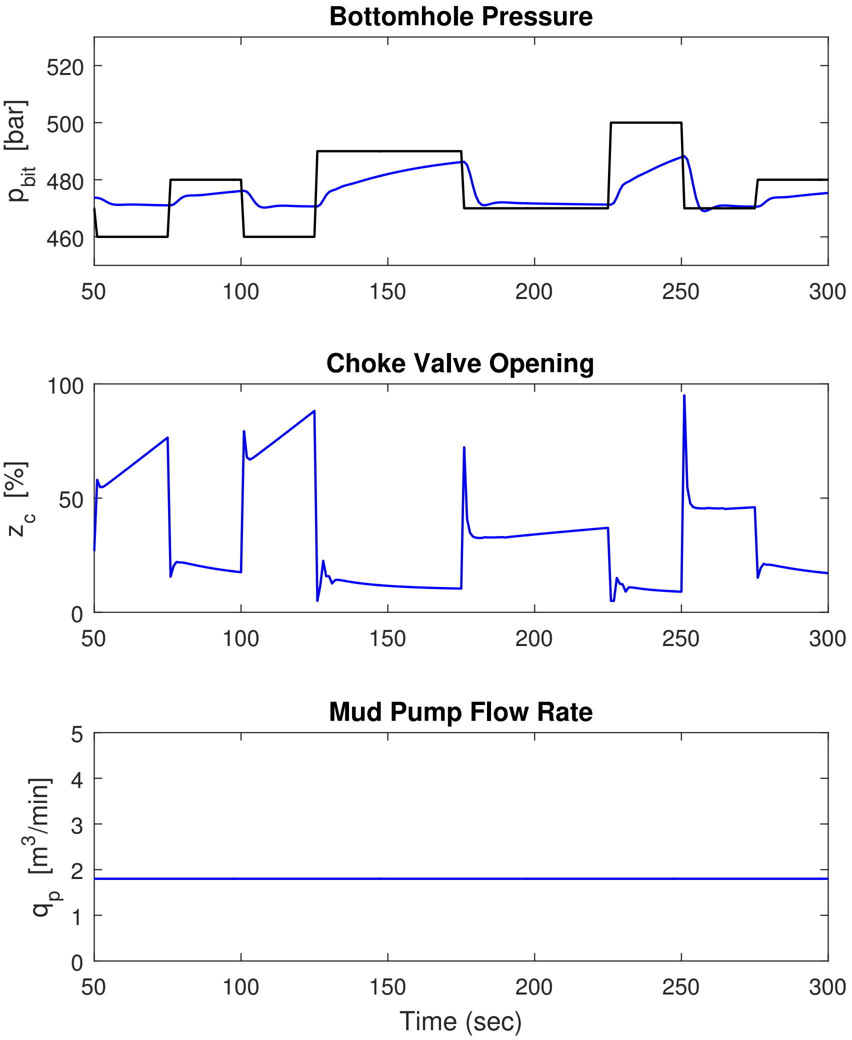

Figure 3.7: BHP control performance during normal drilling - PID

circulation flow through the choke valve. The back pressure pump is included as an MV in the NMPC configuration. Thus, the back pressure pump and choke valve move together and successfully maintain the BHP within ± 1 bar deviation (Figure 3.10). Furthermore, when the mud pump flowrate MV is set to receive a ramp input, NMPC automatically considers it as a process disturbance variable, DV. The NMPC controller includes the change of the DV in the prediction and control calculation. This gives feedforward information that is unavailable to controllers that rely solely on feedback control. To validate nonlinear control of the Hammerstein-Weiner NMPC, the

www.manaraa.com

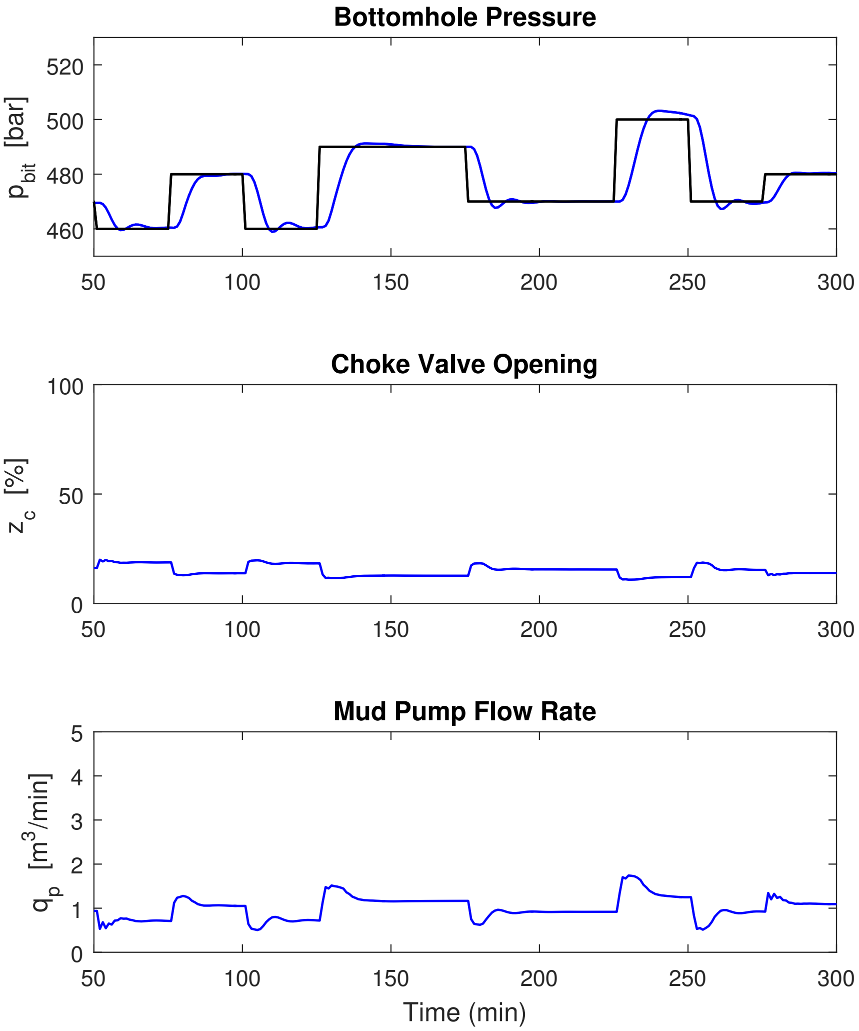

Figure 3.8: BHP control performance during normal drilling - NMPC

pure LMPC control results are compared with the NMPC results in the same plot in Figure 3.10. The LMPC, not including the Hammerstein-Weiner nonlinearity block, shows severe oscillation on both the CVs and MVs when the mud pump flowrate reaches zero. On the contrary, the NMPC shows the appropriate control performance covering the process nonlinearity with the static nonlinear blocks.

Figure 3.11 and 3.12 show the kick attenuation performance of NMPC. The CVs and We-Mod output are shown in Figure 3.11 and MVs of NMPC are displayed in Figure 3.12. The

www.manaraa.com

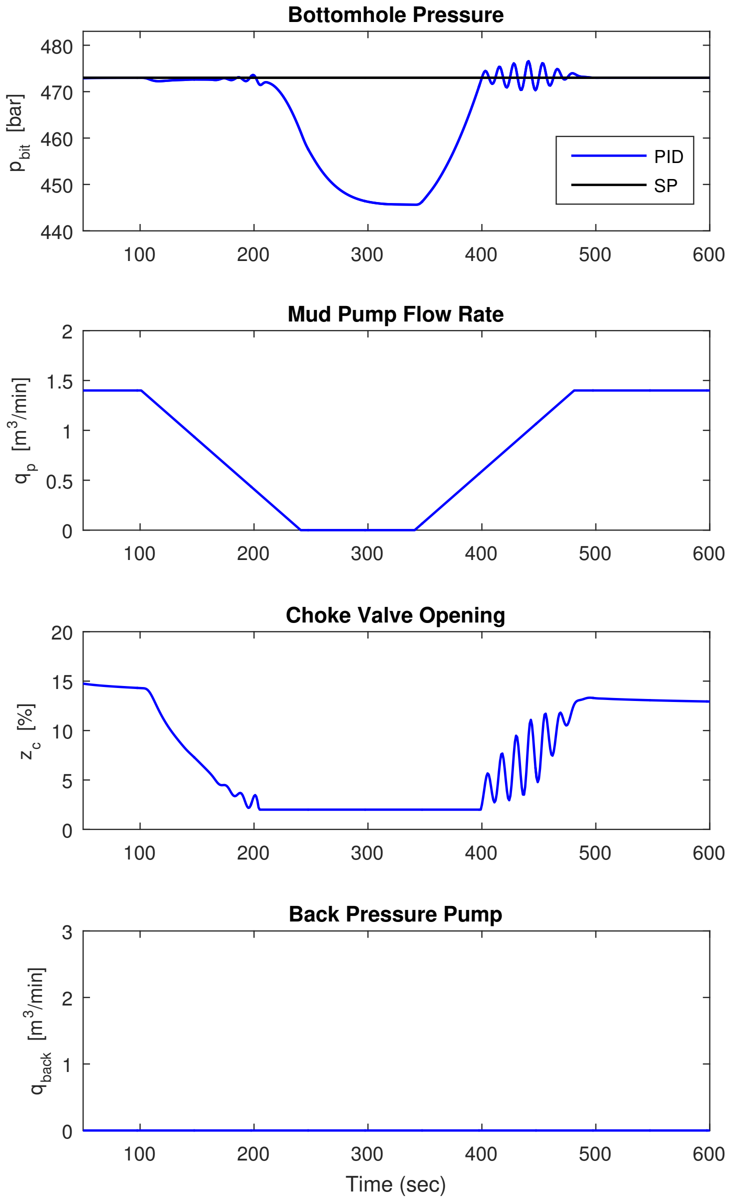

Figure 3.9: BHP control performance during pipe connection - PID

additional CV, flow balance ($q_{bal}$), is added to the existing control matrix that already has BHP as a main CV for normal drilling and pipe connection. Both CVs are turned on at the beginning of the simulation. The control set ranges of the BHP and flow balance are set to ± 1 of 466 bar and

المنارة للاستشارات
www.manaraa.com

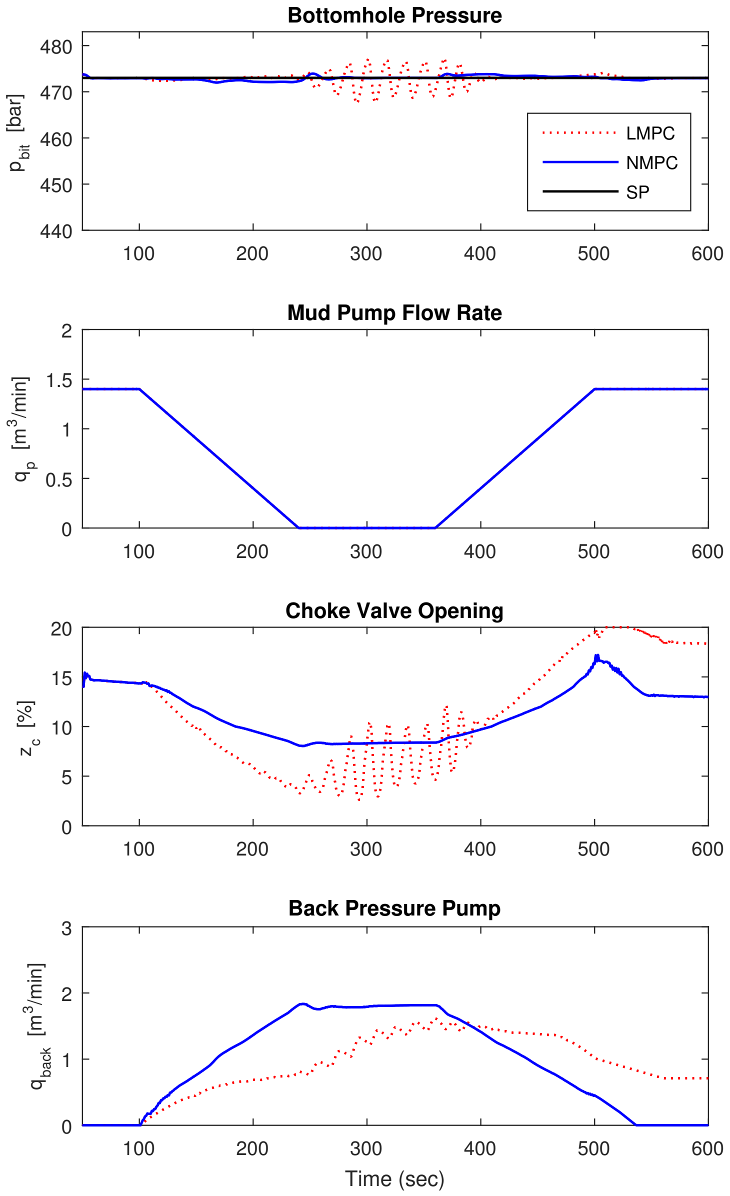

Figure 3.10: BHP control performance during pipe connection - LMPC & NMPC

± 0.01 of 0 m$^3$/min, respectively. New prioritizing limits are applied to both CVs, with the limits for the BHP being relatively narrower than those of the flow balance, as summarized below.

$$\text{Control set range for } p_{bit} = \text{set point for } p_{bit} \pm 1 \text{ bar}$$

$$\text{Control set range for } q_{bal} = \text{set point for } q_{bal} \pm 0.01 \text{ m}^3\text{/min}$$

المنارة للاستشارات
www.manaraa.com

$$\text{Prioritizing limits for } p_{bit} = \text{set point for } p_{bit} \pm 3 \text{ bar}$$

$$\text{Prioritizing limits for } q_{bal} = \text{set point for } q_{bal} \pm 0.5 \text{ m}^3\text{/min}$$

$$\text{where, set point for } p_{bit} = 466 \text{ bar}$$

$$\text{set point for } q_{bal} = 0 \text{ m}^3\text{/min}$$

Both of the CVs (flow balance and BHP) fluctuate as the gas influx starts at 100 seconds. The controller immediately turns off the BHP control letting it increase and stabilize at a new balance condition while attenuating the gas influx with the other CV, flow balance. After the gas influx starts, the BHP steeply increases and goes above the prioritizing limits, while the flow balance is still within prioritizing limits. The controller logic prioritizes flow balance control over BHP control to attenuate the kick. In the results, the controller closes the choke valve and increases both the main mud pump and the back pressure pump, which is anticipated in kick attenuation. These control actions efficiently block the gas migration and increase the wellbore pressure to balance to the new reservoir pressure. Approximately one minute after the kick occurs, BHP is stabilized at 481 bar, stopping the amount of total gas influx at 60 kg. At 180 seconds, the set point of the BHP is adjusted based on the current pressure with an additional safety margin. The BHP is now placed within the prioritizing limits and turned on for future pressure control.

### 3.5 Conclusions

This study proposes an advanced NMPC control algorithm for MPD automation of BHP and flow balance control. The Hammerstein-Wiener based NMPC shows a superior control performance to a conventional PID controller. A number of advantages of NMPC are discussed and validated with common operation scenarios. The proposed method assumes that the bottom hole pressure is measurable by WDP telemetry. The proposed method improves the control reliability by eliminating uncertainties of predictive BHP estimation. By adjusting multiple MVs simultaneously the control performance is significantly improved for normal drilling, pipe stand connections, and in kick attenuation. For the kick attenuation scenario, adding the additional CV and prioritizing limits combines flow balance control and utilizes BHP control when there is no significant flow imbalance.

المنارة للاستشارات
www.manaraa.com

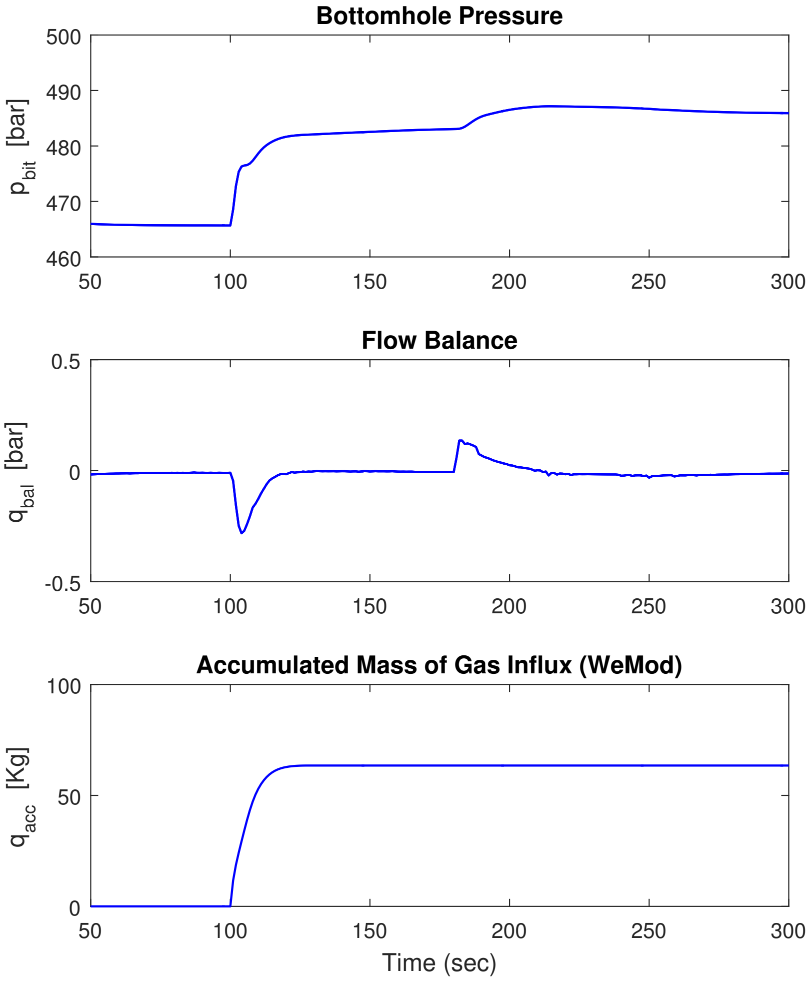

Figure 3.11: BHP control performance during kick attenuation - NMPC (CVs)

المنـــارة للاستشارات
www.manaraa.com

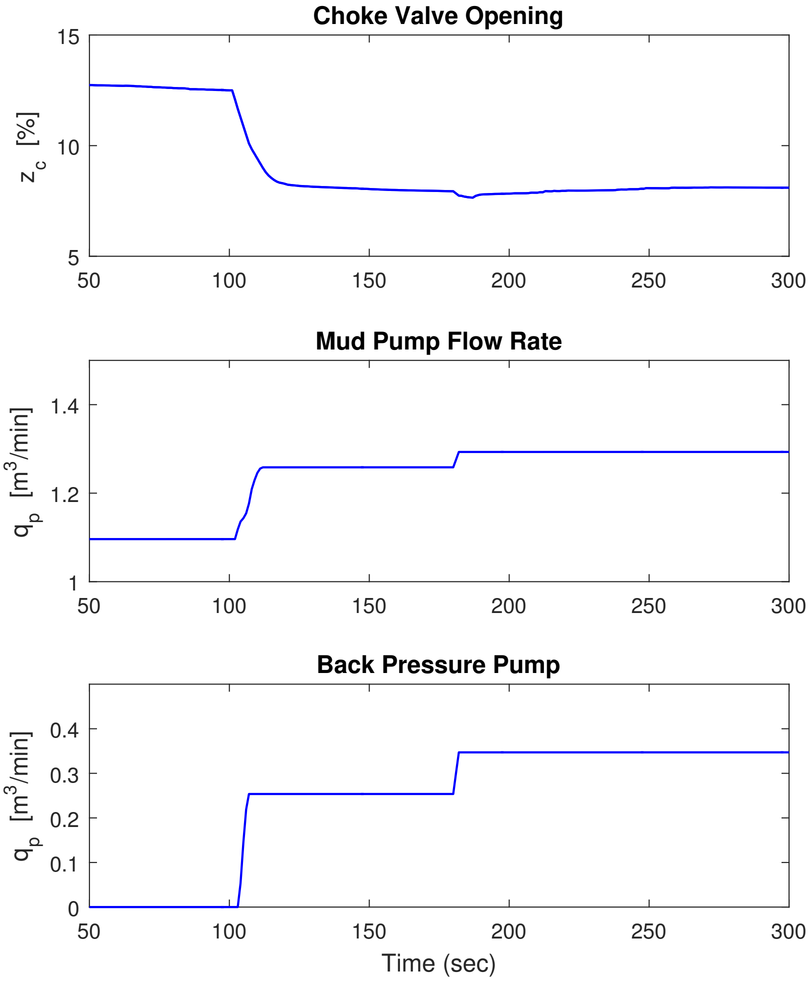

Figure 3.12: BHP control performance during kick attenuation - NMPC (MVs)

www.manaraa.com

# CHAPTER 4. CONCLUSIONS AND FUTURE WORK

## 4.1 Conclusions

MPD and WDP are two significant advances in the drilling industry providing better control of tight pressure limits. MPD gives more adjustable variables in a closed system to have a fast response and precise pressure control. WDP offers real-time communication to bottomhole tools. These two benefits of MPD and WDP open the door for research and development of advanced control systems for drilling operation. As many other industries have already experienced, model-based control and estimation algorithms have the potential to be of significant benefit to the drilling industry. However, unlike in other industries, MPD automation using MPC and MHE is more challenging due to the specific complexities of drilling operations. Current high-fidelity drilling simulators have a large number of variables and parameters that require a large amount of computational power for simulation and these sophisticated simulation models cannot be used directly in optimization. A low-order model captures the main dynamics of the drilling hydraulics and has been used successfully in many drilling automation research projects. The simplified flow model used in this study is more comprehensive than the low-order models because it is a slightly simplified version of an existing high-fidelity model, keeping the most important components but omitting or simplifying those that are less important for BHP control. The other type of model used in this study is a Hammerstein-Wiener model classified as an empirical nonlinear model. This type of model has many benefits in terms of computation time because it consists of linear dynamics and static nonlinear gain blocks. The nonlinear gain blocks manage the nonlinearity of the process by transforming the input or output of linear dynamic model. These nonlinear gain blocks are not included in the optimization problem. Thus, the computational load is similar to that of linear MPC.

المنارة للاستشارات

www.manaraa.com

The objective of this study is to validate the control performance of MPC and MHE by using the two different types of models, SFM and Hammerstein-Winer model in three different test scenarios.

Chapter 2 investigates the BHP control performance of a MPC controller that uses a simplified, physics-based flow model. Full-closed and semi-closed loop control schemes are presented and in each scheme the BHP is shown to be successfully controlled in conditions of normal drilling, pipe connection, and mud density displacement. The results demonstrate tight controller performance that successfully maintained the BHP to within 1 bar of the set point in each scenario. Additionally, MHE is used to calibrate the model and effectively estimates the drill string and annulus friction factors. The effectiveness of the controller is predicated on the quality of the estimator, and the present study demonstrates that tight BHP control can be achieved in conjunction with estimation of the unknown model parameters, $f_a$ and $f_d$.

In normal drilling scenarios, the BHP can be controlled and changed to a desired setpoint. Control is improved with a full-closed control scheme, but the advantages over a semi-closed loop are marginal. Similarly, when controlling BHP during pipe connections, it is more effective to use a full-closed loop, but the semi-closed loop is also successful. Inclusion of feed forward control in the MPC algorithm enabled effective BHP control in this scenario. It is observed that model mismatch is introduced by the pipe connection when using a semi-closed loop, and model recalibration should be performed after such a procedure. In mud density displacement the semi-closed loop again develops some mismatch that would be best remedied by a model recalibration, but the mismatch is minimal and the recalibration does not need to immediately follow a period of mud density displacement. The full-closed scheme again proves more effective than the semi-closed scheme for mud density displacement.

The MPC controller handled the several scenarios successfully and the results indicate that a simplified model has the potential to achieve BHP control and such a model would be effective. The data shows that the differences between full-closed loop and semi-closed control schemes is minimal. The results of this study solidify the utility of SFM in MPD. A SFM can be a useful tool for controlling systems using mud pulsing or WDP, and such control comes at a smaller computational cost than use of a HFM and offers the benefit of tight control that improves drilling quality as well as the opportunity to drill more complex wells that have narrow pressure margins.

المنارة للاستشارات
www.manaraa.com

Chapter 3 proposes an advanced NMPC control algorithm for MPD automation of BHP and flow balance control. The Hammerstein-Wiener based NMPC shows a superior control performance to a conventional PID controller. A number of advantages of NMPC are discussed and validated with three operation scenarios. The proposed method assumes that the bottom hole pressure is measurable by WDP telemetry. The proposed method improves the control reliability by eliminating uncertainties of predictive BHP estimation. By adjusting multiple MVs simultaneously the control performance is significantly improved for normal drilling, pipe stand connections, and in kick attentuation. For the kick attenuation scenario, adding the additional CV and prioritizing limits combines flow balance control and utilizes BHP control when there is no significant flow imbalance.

In a first scenario, the performance of set point tracking during normal drilling operation is compared. By changing the set point of the BHP, the conventional controller manipulates only the choke valve opening while the nonlinear controller moves choke valve opening, mud pump, and back pressure pump simultaneously. In a second scenario, a pipe connection of a typical drillpipe stand is demonstrated. The conventional controller is not able to regulate the BHP by adjusting the choke valve only. Although a linear version of the controller is able to exploit multivariable relationships, absence of the nonlinear relationships results in severe oscillation when the operational range is shifted outside of the training region. The nonlinear controller maintains a BHP within 1 bar of the requested set point. A third scenario investigates the kick attenuation performance of conventional and nonlinear control algorithms. The nonlinear controller attenuates the kick within well control conditions without requiring a well shut-in procedure.

## 4.2 Future Work

1. Develop a mud mixing automation system

   Mud density is one possible adjustable variable for BHP control. Most BHP control research focuses on using the choke valve, main mud pump, and back pressure pump as a fast and effective manipulated variables. Although the mud properties have a slow response time for BHP control, eliminating the manual mud mixing time can allow the mud density make additional contributions to the control scheme. Developing the simplified model with an

المنارة للاستشارات
www.manaraa.com

enhanced mud property portion and combining it with the existing BHP control systems is suggested for a future research topic.

2. Deploy a simplified drillstring dynamics model for real-time automation and optimization
   The empirical drill string dynamics model has been used for combined ROP and BHP control. ROP can be improved by minimizing the BHP. It is necessary to use or develop the physics based drill string dynamics model to include an elaborate bit/rock interaction model to have a better understanding of the relationship between BHP and ROP. This work would also expand case studies for hole cleaning and cuttings build-up control by combining the hydraulics model with a drilling dynamics model for a multivariable drilling automation system.

المنارة للاستشارات
www.manaraa.com

# REFERENCES

[1] Fredericks, P. D., Reitsma, D., Runggai, T., Hudson, J. N., Zaeper, R., Backhaus, O., and Hernandez, M., 2008. “Successful implementation of first closed loop, multiservice control system for automated pressure management in a shallow gas well offshore Myanmar.” In *SPE/IADC*, Society of Petroleum Engineers, SPE-112651-MS. 6

[2] Breyholtz, O., Nygaard, G., and Nikolaou, M., 2010. “Automatic control of managed pressure drilling.” In *2010 American Control Conference, ACC 2010, June 30, 2010 - July 2, 2010*, Proceedings of the 2010 American Control Conference, ACC 2010, IEEE Computer Society, pp. 442–447. 6

[3] Geehan, T., and Zamora, M., 2010. “Automation of well construction fluids domain.” In *IADC/SPE Drilling Conference and Exhibition*, Society of Petroleum Engineers, SPE-128903-MS. 6

[4] Godhavn, J.-M., Pavlov, A., Kaasa, G.-O., and Rolland, N. L., 2011. “Drilling seeking automatic control solutions.” In *18th IFAC World Congress, August 28, 2011 - September 2, 2011*, Vol. 18 of *IFAC Proceedings Volumes (IFAC-PapersOnline)*, IFAC Secretariat, pp. 10842–10850. 6, 11

[5] Rasmus, J., Dorel, A., Azizi, T., David, A., Duran, E., Lopez, H., Aguinaga, G., Beltran, J. C., Ospino, A., and Ochoa, E., 2013. “Utilizing wired drill pipe technology during managed pressure drilling operations to maintain direction control, constant bottom-hole pressures, and well-bore integrity in a deep, ultra-depleted reservoir.” In *SPE/IADC Drilling*, Society of Petroleum Engineers, SPE-163501-MS. 6

[6] Stamnes, O. N., Kaasa, G.-O., and Aamo, O. M., 2011. “Adaptive estimation of downhole pressure for managed pressure drilling operations.” In *2011 IEEE International Symposium on Intelligent Control, ISIC 2011, September 28, 2011 - September 30, 2011*, IEEE International Symposium on Intelligent Control - Proceedings, Institute of Electrical and Electronics Engineers Inc., pp. 989–995. 6, 11

[7] Mansour, A. M., Gordon, B. J., Ling, Q., and Shen, Q., 2013. “TLP survivability against progressive failure of tendon and foundation systems in offshore western Australian harsh environment.” p. V001T01A079. 6

[8] Eaton, A. N., Beal, L. D. R., Thorpe, S. D., Hubbell, C. B., Hedengren, J. D., Nybø, R., and Aghito, M., 2017. “Real time model identification using multi-fidelity models in managed pressure drilling.” *Computers and Chemical Engineering,* **97**, pp. 76–84. 7, 15

المنارة للاستشارات

www.manaraa.com

[9] Sugiura, J., Samuel, R., Oppelt, J., Ostermeyer, G. P., Hedengren, J., and Pastusek, P., 2015. “Drilling modeling and simulation: Current state and future goals.” In *SPE/IADC Drilling Conference and Exhibition*, Society of Petroleum Engineers, SPE-173045-MS. 7

[10] Poletto, F., and Miranda, F., 2004. *Seismic while drilling: Fundamentals of drill-bit seismic for exploration*., Vol. 35 Elsevier. 7

[11] Pixton, D., and Craig, A., 2014. “Drillstring network 2.0: An enhanced drillstring network based on 100 wells of experience.” In *IADC/SPE Drilling Conference and Exhibition*, Society of Petroleum Engineers, SPE-167965-MS. 8

[12] Long, R., and Veeningen, D., 2011. “Networked drill pipe offers along-string pressure evaluation in real time.” *World oil,* **232**(9), pp. 91–94. 8

[13] Lee, J. H., and Ricker, N. L., 1994. “Extended Kalman filter based nonlinear model predictive control.” *Industrial & Engineering Chemistry Research,* **33**(6), pp. 1530–1541. 9

[14] Ahn, S.-M., Park, M.-J., and Rhee, H.-K., 1999. “Extended Kalman filter-based nonlinear model predictive control for a continuous mma polymerization reactor.” *Industrial & engineering chemistry research,* **38**(10), pp. 3942–3949. 9

[15] Hedengren, J. D., and Eaton, A. N., 2017. “Overview of estimation methods for industrial dynamic systems.” *Optimization and Engineering,* **18**(1), pp. 155–178. 9

[16] Rao, C. V., and Rawlings, J. B., 2000. *Nonlinear moving horizon state estimation*. Springer, pp. 45–69. 9

[17] Rao, C. V., Rawlings, J. B., and Mayne, D. Q., 2003. “Constrained state estimation for nonlinear discrete-time systems: Stability and moving horizon approximations.” *IEEE transactions on automatic control,* **48**(2), pp. 246–258. 9

[18] Rawlings, J. B., 2013. “Moving horizon estimation.” *Encyclopedia of Systems and Control*, pp. 1–7. 9

[19] Nygaard, G., Naedal, G., and Mylvaganam, S., 2006. “Evaluating nonlinear Kalman filters for parameter estimation in reservoirs during petroleum well drilling.” In *Computer Aided Control System Design, 2006 IEEE International Conference on Control Applications, 2006 IEEE International Symposium on Intelligent Control, 2006 IEEE*, IEEE, pp. 1777–1782. 10

[20] Asgharzadeh Shishavan, R., Hubbell, C., Perez, H., Hedengren, J., and Pixton, D., 2015. “Combined rate of penetration and pressure regulation for drilling optimization by use of high-speed telemetry.” *SPE Drilling & Completion, SPE-170275-PA*. 10, 14, 37

[21] Asgharzadeh Shishavan, R., Hubbell, C., Perez, H. D., Hedengren, J. D., Pixton, D. S., and Pink, A. P., 2016. “Multivariate control for managed-pressure-drilling systems by use of high-speed telemetry.” *Society of Petroleum Engineers, SPE-170962-PA*. 10, 11, 37, 47

[22] Nikoofard, A., Johansen, T. A., and Kaasa, G.-O., 2014. “Nonlinear moving horizon observer for estimation of states and parameters in under-balanced drilling operations.” In *ASME 2014 Dynamic Systems and Control Conference*, American Society of Mechanical Engineers, pp. V003T37A002–V003T37A002. 10

المنارة للاستشارات

www.manaraa.com

[23] Nikoofard, A., Aarsnes, U. J. F., Johansen, T. A., and Kaasa, G.-O., 2015. “Estimation of states and parameters of a drift-flux model with unscented Kalman filter.” *IFAC-PapersOnLine,* **48**(6), pp. 165–170. 10

[24] Qin, S. J., and Badgwell, T. A., 2003. “A survey of industrial model predictive control technology.” *Control Engineering Practice,* **11**(7), pp. 733–764. 10, 14, 15, 36

[25] Allgöwer, F., Badgwell, T. A., Qin, J. S., Rawlings, J. B., and Wright, S. J., 1999. *Nonlinear predictive control and moving horizon estimationan introductory overview*. Springer, pp. 391–449. 10

[26] Pedersen, T., and Godhavn, J.-M., 2013. “Model predictive control of flow and pressure in underbalanced drilling.” *IFAC Proceedings Volumes,* **46**(32), pp. 307–312. 10, 11

[27] Møgster, J., Godhavn, J.-M., and Imsland, L., 2013. “Using mpc for managed pressure drilling.” *Modeling, Identification and Control,* **34**(3), p. 131. 10, 11

[28] Siahaan, H. B., and Nygaard, G., 2008. “On modeling and observer design of fluid flow dynamics for petroleum drilling operations.” In *47th IEEE Conference on Decision and Control, CDC 2008, December 9, 2008 - December 11, 2008*, Proceedings of the IEEE Conference on Decision and Control, Institute of Electrical and Electronics Engineers Inc., pp. 1857–1863. 10, 11, 15, 37

[29] Nygaard, G. H., Imsland, L. S., and Johannessen, E. A., 2007. “Using NMPC based on a low-order model for controlling pressure during oil well drilling.” In *8th International IFAC Symposium on Dynamics and Control of Process Systems*. 11

[30] Zhou, J., Stamnes, O. N., Aamo, O. M., and Kaasa, G.-O., 2011. “Switched control for pressure regulation and kick attenuation in a managed pressure drilling system.” *IEEE Transactions on Control Systems Technology,* **19**(2), pp. 337–350. 11, 47

[31] Carlsen, L. A., Nygaard, G., and Nikolaou, M., 2013. “Evaluation of control methods for drilling operations with unexpected gas influx.” *Journal of Process Control,* **23**(3), pp. 306–316. 11

[32] Nygaard, G., and Nvdal, G., 2006. “Nonlinear model predictive control scheme for stabilizing annulus pressure during oil well drilling.” *Journal of Process Control,* **16**(7), pp. 719–732. 11, 15, 37

[33] Nygaard, G., and Nvdal, G., 2005. “Modelling two-phase flow for control design in oil well drilling.” In *2005 IEEE International Conference on Control Applications, CCA, August 28, 2005 - August 31, 2005*, Proceedings of the IEEE International Conference on Control Applications, Institute of Electrical and Electronics Engineers Inc., pp. 675–680. 11, 15, 37

[34] Nygaard, G., Nvdal, G., and Mylvaganam, S., 2007. “Evaluating nonlinear Kalman filters for parameter estimation in reservoirs during petroleum well drilling.” In *Joint 2006 IEEE Conference on Control Applications (CCA), Computer-Aided Control Systems Design Symposium (CACSD) and International Symposium on Intelligent Control (ISIC), October 4, 2006 - October 6, 2006*, Proceedings of the IEEE International Conference on Control Applications, Institute of Electrical and Electronics Engineers Inc., pp. 1777–1782. 11

المنارة للاستشارات

www.manaraa.com

[35] Storkaas, E., Skogestad, S., and Godhavn, J. M., 2003. “A low-dimensional dynamic model of severe slugging for control design and analysis.” In *11th International Conference on Multiphase 03: Extending the Boundaries of Flow Assurance, June 11, 2003 - June 13, 2003*, International Conference on Multiphase: Extending the Boundaries of Flow Assurance, BHR Group Limited, pp. 117–133. 11

[36] Nazari, T., Mostafavi, V., and Hareland, G., 2009. “UKF-based estimation fusion of underbalanced drilling process using pressure sensors.” In *2009 IEEE Intrumentation and Measurement Technology Conference, I2MTC 2009, May 5, 2009 - May 7, 2009*, 2009 IEEE Intrumentation and Measurement Technology Conference, I2MTC 2009, IEEE Computer Society, pp. 1012–1017. 11

[37] Kaasa, G.-O., Stamnes, Ø. N., Aamo, O. M., and Imsland, L. S., 2012. “Simplified hydraulics model used for intelligent estimation of downhole pressure for a managed-pressure-drilling control system.” *SPE Drilling & Completion, SPE-143097-PA*. 11, 15, 37

[38] Tennøy, S., Neæsheim, L., and Nygaard, G., 2012. Iris drill for matlab win7 users guide Report, International Research Institute of Stavanger. 11

[39] Hedengren, J. D., Shishavan, R. A., Powell, K. M., and Edgar, T. F., 2014. “Nonlinear modeling, estimation and predictive control in apmonitor.” *Computers & Chemical Engineering,* **70**, pp. 133–148. 11, 41

[40] McLennan, J., Institute, G. R., and Gas Research Institute. Chicago, I., 1997. *Underbalanced Drilling Manual*. Gas Research Institute. 14, 37, 44

[41] Pixton, D. S., Asgharzadeh Shishavan, R., Perez, H. D., Hedengren, J. D., and Craig, A., 2014. “Addressing ubo and mpd challenges with wired drill pipe telemetry.” Series Addressing UBO and MPD Challenges with Wired Drill Pipe Telemetry, Society of Petroleum Engineers, SPE-168953-MS. 15, 43

[42] Park, J., Webber, T., Shishavan, R. A., and Hedengren, J. D., 2017. “Improved bottomhole pressure control with wired drillpipe and physics-based models.” In *SPE/IADC Drilling Conference and Exhibition*, Society of Petroleum Engineers, SPE-184610-MS. 15

[43] Landet, I. S., Pavlov, A., and Aamo, O. M., 2013. “Modeling and control of heave-induced pressure fluctuations in managed pressure drilling.” *IEEE Transactions on Control Systems Technology,* **21**(4), pp. 1340–1351. 15

[44] El Boubsi, R., Andresen, J. A., van Og, G., Bjørkevoll, K. S., Nybø, R., Brevik, J. O., Nygaard, G., and Smith, G. G., 2017. “Demo2000 - drilling mud process control.” In *SPE Bergen One Day Seminar*, Society of Petroleum Engineers, SPE-185929-MS. 15

[45] Stamnes, . N., 2007. “Adaptive observer for bottomhole pressure during drilling.” Thesis, NTNU. 18

[46] Stamnes, O. N., Zhou, J., Kaasa, G.-O., and Aamo, O. M., 2008. “Adaptive observer design for the bottomhole pressure of a managed pressure drilling system.” In *47th IEEE Conference on Decision and Control, CDC 2008, December 9, 2008 - December 11, 2008*, Proceedings

المنارة للاستشارات
www.manaraa.com

of the IEEE Conference on Decision and Control, Institute of Electrical and Electronics Engineers Inc., pp. 2961–2966. 18, 24, 46

[47] Zhou, J., Nygaard, G., Godhavn, J.-M., Breyholtz, O., and Vefring, E. H., 2010. “Adaptive observer for kick detection and switched control for bottomhole pressure regulation and kick attenuation during managed pressure drilling.” In *2010 American Control Conference, ACC 2010, June 30, 2010 - July 2, 2010*, IEEE Computer Society, pp. 3765–3770. 18

[48] Ławryńczuk, M., 2013. “Practical nonlinear predictive control algorithms for neural wiener models.” *Journal of Process Control,* **23**(5), pp. 696–714. 38

[49] Ławryńczuk, M., 2015. “Nonlinear predictive control for Hammersteinwiener systems.” *ISA Transactions,* **55**, pp. 49–62. 38

[50] Jeong, B.-G., Yoo, K.-Y., and Rhee, H.-K., 2001. “Nonlinear model predictive control using a wiener model of a continuous methyl methacrylate polymerization reactor.” *Industrial & engineering chemistry research,* **40**(25), pp. 5968–5977. 38

[51] Ramesh, K., Hisyam, A., Aziz, N., and Shukor, S. A., 2012. “Nonlinear model predictive control of a distillation column using wavenet based Hammerstein model.” *Engineering Letters,* **20**(4), pp. 1–6. 38

[52] Abdennour, R., Ksouri, M., and M’Sahli, F., 2002. “Nonlinear model-based predictive control using a generalised Hammerstein model and its application to a semi-batch reactor.” *The International Journal of Advanced Manufacturing Technology,* **20**(11), pp. 844–852. 38

[53] Huo, H.-B., Zhu, X.-J., Hu, W.-Q., Tu, H.-Y., Li, J., and Yang, J., 2008. “Nonlinear model predictive control of sofc based on a Hammerstein model.” *Journal of Power Sources,* **185**(1), pp. 338–344. 38

[54] Sung, S. W., 2002. “System identification method for Hammerstein processes.” *Industrial & Engineering Chemistry Research,* **41**(17), pp. 4295–4302. 38

[55] Eskinat, E., Johnson, S. H., and Luyben, W. L., 1991. “Use of Hammerstein models in identification of nonlinear systems.” *AIChE Journal,* **37**(2), pp. 255–268. 38

[56] Wills, A., Schön, T. B., Ljung, L., and Ninness, B., 2013. “Identification of Hammerstein-Wiener models.” *Automatica,* **49**(1), pp. 70–81. 38

[57] Beal, L. D., Park, J., Petersen, D., Warnick, S., and Hedengren, J. D., 2017. “Combined model predictive control and scheduling with dominant time constant compensation.” *Computers & Chemical Engineering,* **104**, pp. 271–282. 38

[58] Fruzzetti, K., Palazolu, a., and McDonald, K., 1997. “Nonlinear model predictive control using Hammerstein models.” *Journal of Process Control,* **7**, pp. 31–41. 38

[59] Norquay, S. J., Palazoglu, A., and Romagnoli, J., 1998. “Model predictive control based on wiener models.” *Chemical Engineering Science,* **53**(1), pp. 75–84. 38

[60] Gravdal, J. E., Lorentzen, R. J., and Time, R. W., 2010. “Wired drill pipe telemetry enables real-time evaluation of kick during managed pressure drilling.” In *SPE Asia Pacific Oil*

المنارة للاستشارات
www.manaraa.com

*and Gas Conference and Exhibition 2010, APOGCE 2010, October 18, 2010 - October 20, 2010*, Vol. 1 of *Society of Petroleum Engineers - SPE Asia Pacific Oil and Gas Conference and Exhibition 2010, APOGCE 2010*, Society of Petroleum Engineers, SPE-132989-MS, pp. 582–601. 43

www.manaraa.com

# APPENDIX A. OBJECTIVE FUNCTIONS OF MPC AND MHE

## A.1 QP objective function for MHE

$$\min_{\Delta p} \Phi = \sum_{i=1}^{N} [(y_{p,k-N+i|k} - y_{m,k-N+i|k})^T W (y_{p,k-N+i|k} - y_{m,k-N+i|k}) + (\Delta p^T_{k-N+i|k} V \Delta p_{k-N+i|k})] \tag{A.1}$$

$$where, \Delta p_{k-N+i|k} = p_{k-N+i|k} - p_{k-N+i-1|k} \tag{A.2}$$

$$s.t.\;\; 0 = f(\dot{x}, x, y, p, d, u) \tag{A.3}$$

$$0 = g(x, y, p, d, u) \tag{A.4}$$

$$0 \le h(x, y, p, d, u) \tag{A.5}$$

Table A.1: Summary of parameters used in QP objective function for MHE

| **Parameter** | **Description** |
|---|---|
| $\Phi$ | Objective function |
| $N$ | Horizon length for MHE |
| $k$ | Current time step |
| $y_p, y_m$ | Measured CV value ($y_p$) and model result of CV value ($y_m$) |
| $V, W$ | Weighting Matrices for CVs and parameters |
| $u, x, p, d$ | Model inputs($u$), states($x$), parameters($p$), and disturbance($d$) |
| $f, g, h$ | Model equation ($f$), output function ($g$), and inequality constraints ($h$) |

المنارة للاستشارات
www.manaraa.com

## A.2 QP objective function for MPC

$$\min_{\Delta u} \Phi = \sum_{i=1}^{N} [(\hat{y}_{k+i|k} - \hat{y}_t)^T Q (\hat{y}_{k+i|k} - \hat{y}_t)] + \sum_{j=1}^{M} (\Delta u_{k+j|k}^T R \Delta u_{k+j|k}) \tag{A.6}$$

$$where, \Delta u_{k+j|k} = u_{k+j+1|k} - u_{k+j|k} \tag{A.7}$$

$$s.t. \;\; 0 = f(\dot{x}, x, y, p, d, u) \tag{A.8}$$

$$0 = g(x, y, p, d, u) \tag{A.9}$$

$$0 \leq h(x, y, p, d, u) \tag{A.10}$$

$$\tau_c \frac{dy_t}{dt} + y_t = sp \tag{A.11}$$

Table A.2: Summary of parameters used in QP objective function for MPC

| **Parameter** | **Description** |
|---|---|
| $\Phi$ | Objective function |
| $N, M$ | Prediction horizon($N$), Control horizon($M$) |
| $k$ | Current time step |
| $\hat{y}$ | Predicted CV value of dynamic model |
| $\hat{y}_t$ | Desired set point trajectory in the prediction horizon |
| $Q, R$ | Weighting Matrices for CVs and MVs |
| $sp$ | Set point in the prediction horizon |
| $u, x, p, d$ | Model inputs($u$), states($x$), parameters($p$), and disturbance($d$) |
| $f, g, h$ | Model equation ($f$), output function ($g$), and inequality constraints ($h$) |
| $\tau_c$ | Time constant of desired controlled variable response |

المنارة للاستشارات

www.manaraa.com

# APPENDIX B. PYTHON CODE FOR SFM MPC AND MHE

## B.1 Master Code

```
### IMPORTS ###
import well_model
import sfm_mhe
import sfm_mpc
import numpy as np
import datetime as dt
import matplotlib.pyplot as plt
import time as tme

start_time = tme.time()

timeStep = 5   # seconds
n = 240        # number of timesteps

# Define horizons
H = 5 # Estimation Horizon for MHE
P = 5 # Prediction Horizon for MPC

# Define time vector for simulation [Days]
TimeStart = dt.datetime.now() # find current date
# Convert to Excel Format ( Difference in days since 1/1/1900)
Begin = dt.datetime(1899,12,30)
delta = TimeStart - Begin
TimeStart = float(delta.days) + (float(delta.seconds) / 86400)
```

المنارة للاستشارات
www.manaraa.com

```
TimeStep = float(timeStep) / (24 * 60 * 60) # conversion to days

### Arrays for storing data ###
time       = np.zeros(n)
bitposition = np.zeros(n)
p_bit_hfm = np.zeros(n)
p_bit_sfm = np.zeros(n)
spp_hfm = np.zeros(n)
spp_sfm = np.zeros(n)
mud_flow_in = np.zeros(n)
mud_flow_out_hfm = np.zeros(n)
mud_flow_out_sfm = np.zeros(n)
choke_pressure_input = np.zeros(n)
choke_pressure_hfm = np.zeros(n)
choke_pressure_sfm = np.zeros(n)
friction_d_hfm = np.zeros(n) # hfm friction for drillstring
friction_a_hfm = np.zeros(n) # hfm friction for Annulus
friction_d_sfm = np.zeros(n) # sfm friction for drillstring
friction_a_sfm = np.zeros(n) # sfm friction for Annulus
SP = np.zeros(n)

class data_input_class():
    TimeStep = TimeStep
    time = TimeStart
    bitposition = 3765.    # [m]
    depthhole = 3765.      # [m]
    rotary_speed = 100.    # [rpm]
    ROP = 0.               # [m/hr]
    mudflowin = 1000.      # [m^3/s]
    mud_density_in = 1.5   # [sg]
    desired_emw = 1.5      # [sg]
    choke_press = 23.      # [bar]
```

المنارة للاستشارات
www.manaraa.com

```
    cross_flow = 0         # [lpm]
    input_mud_temp = 50.   # [degC]
    set_point_position = 3765.  # [m]
    friction_d = 1.0       # friction for Drillstring
    friction_a = 1.0       # friction for Annulus
    mhe_sw = 0          # switch for mhe
    mpc_sw = 0          # switch for mpc
    SV1_sw = 0          # switch for BHP
    SV2_sw = 0          # switch for SPP
    FV1_sw = 0          # switch for f_a
    FV2_sw = 0          # switch for f_d
    SP = 313            # setpoint

well_input = data_input_class()
mhe_input = data_input_class()
mpc_input = data_input_class()

for k in range (0,n): # k = current timestep
    ### Update values to be sent into the well
    Time = TimeStart + TimeStep*k
    well_input.time = Time
    well_input.bitposition = well_input.bitposition +
        (TimeStep*24.)*well_input.ROP
    bitposition[k] = well_input.bitposition
    well_input.depthhole = well_input.bitposition

    ## Model Calibration
    if k == 0:
        well_input.friction_a = 1.1

    if k == 20:
        mhe_input.mhe_sw = 1
```

المنارة للاستشارات
www.manaraa.com

```
    mhe_input.SV1_sw = 1
    mhe_input.SV2_sw = 0
    mhe_input.FV1_sw = 1
    mhe_input.FV2_sw = 0

if k == 30:
    mhe_input.mhe_sw = 1
    mhe_input.SV1_sw = 0
    mhe_input.SV2_sw = 1
    mhe_input.FV1_sw = 0
    mhe_input.FV2_sw = 1

## Start Control
if k == 50:
    mhe_input.mhe_sw = 1
    mhe_input.SV1_sw = 1
    mhe_input.SV2_sw = 1
    mhe_input.FV1_sw = 1
    mhe_input.FV2_sw = 1
    mpc_input.SP = 313
    mpc_input.mpc_sw = 1

if k == 60:
    mpc_input.SP = 320

if k == 100:
    mpc_input.SP = 300

if k == 140:
    mpc_input.SP = 315

sfm_mhe.sfm_save()
```

المنارة للاستشارات

www.manaraa.com

```
sfm_mpc.sfm_save()

### Run estimator
e_ig = np.array([mhe_input.friction_a, mhe_input.friction_d])

if k > H and mhe_input.mhe_sw==1:
    ctlr_moves = np.array([choke_pressure_input[k-H:k],
                         mud_flow_in[k-H:k]])

    measured = np.array([p_bit_hfm[k-H:k],
                      spp_hfm[k-H:k],
                      friction_a_sfm[k-H:k],
                      friction_d_sfm[k-H:k]])

    estimator_out = sfm_mhe.estimate(e_ig, well_input, mhe_input, measured,
       ctlr_moves, H, k)

    mhe_input.friction_a = estimator_out[0]
    mhe_input.friction_d = estimator_out[1]

else:
    e_ig = [mhe_input.friction_a, mhe_input.friction_d]
    estimator_out = e_ig

mpc_input = mhe_input

### Run controller
q_p_hat0 = (np.zeros(P) + well_input.mudflowin)
p_c_hat0 = (np.zeros(P) + well_input.choke_press)
x_ig = np.row_stack((p_c_hat0,q_p_hat0))

control_out = sfm_mpc.control(x_ig, well_input, mpc_input, P, k)
```

www.manaraa.com

```
well_input.mudflowin=control_out[1,0]
well_input.choke_press=control_out[0,0]

well_input.time = Time

sfm_mhe.sfm_load()
sfm_mpc.sfm_load()

## Run well
well_meas = well_model.well_run(well_input)

## Run sfm for MHE
mhe_meas = sfm_mhe.mhe_run(well_input,mhe_input,e_ig,H)

## Run sfm for MPC
mpc_meas = sfm_mpc.mpc_run(mhe_input)

### Store Data
time[k] = (well_input.time-TimeStart)*24*60*60
mud_flow_in[k] = well_input.mudflowin
mud_flow_out_hfm[k] = well_meas.flowout_well *60000.
choke_pressure_input[k] = well_input.choke_press
choke_pressure_hfm[k] = well_meas.p_c
choke_pressure_sfm[k] = mhe_meas.p_c
p_bit_hfm[k] = well_meas.p_bit
p_bit_sfm[k] = mhe_meas.p_bit
spp_hfm[k] = well_meas.spp/1.0e5  # [bar]
spp_sfm[k] = mhe_meas.spp
friction_a_sfm[k] = estimator_out[0]
friction_d_sfm[k] = estimator_out[1]
friction_a_hfm[k] = well_input.friction_a
```

www.manaraa.com

```
    friction_d_hfm[k] = well_input.friction_d
    SP[k] = mpc_input.SP

    print "p_bit HFM, SFM:", [k, round(p_bit_hfm[k],2), round(p_bit_sfm[k],2)]

elapsed_time = tme.time() - start_time
print "Time Elapsed: ",elapsed_time,"seconds"

## plotting
plt.figure(0,figsize=(7,5))
plt.subplot(211)
plt.plot(time[H+2:n],p_bit_hfm[H+2:n],’r--’,lw=2, label=’HFM’)
plt.plot(time[H+2:n],p_bit_sfm[H+2:n],’b-’,lw=2, label=’SFM’)
plt.plot(time[H+2:n],SP[H+2:n],’r-’,lw=2, label=’SP’)
plt.axis([0,n*timeStep,np.floor(np.min(p_bit_sfm))-5,np.ceil(np.max(p_bit_sfm))+5])
plt.legend(loc=4,fontsize=14)
plt.xticks(fontsize=12)
plt.yticks(fontsize=12)
plt.ylabel(’BHP (bar)’,fontsize=14)

plt.subplot(212)
plt.plot(time[H+2:n],spp_hfm[H+2:n],’r--’,lw=2,label=’HFM’)
plt.plot(time[H+2:n],spp_sfm[H+2:n],’b-’,lw=2,label=’SFM’)
plt.axis([0,n*timeStep,np.floor(np.min(spp_sfm))-5,np.ceil(np.max(spp_sfm))+5])
plt.xlabel(’Time (s)’,fontsize=14)
plt.ylabel(’SPP (bar)’,fontsize=14)
plt.xticks(fontsize=12)
plt.yticks(fontsize=12)
plt.legend(loc=4,fontsize=14)

plt.savefig(’MPC1.png’, format=’png’, dpi=400, bbox_inches=’tight’)
plt.savefig(’MPC1.eps’, format=’eps’, dpi=400, bbox_inches=’tight’)
```

المنارة للاستشارات
www.manaraa.com

```
plt.figure(1,figsize=(7,8))
plt.subplot(411)
plt.plot(time[H+2:n],friction_a_sfm[H+2:n], ’b-’,lw=2,label=’SFM’)
plt.axis([0,n*timeStep,min(friction_a_sfm)-0.1,max(friction_a_sfm)+0.1])
plt.legend(loc=4,fontsize=14)
plt.xticks(fontsize=12)
plt.yticks(fontsize=12)
plt.ylabel(’f$_{a}$’,fontsize=14)

plt.subplot(412)
plt.plot(time[H+2:n],friction_d_sfm[H+2:n], ’b-’,lw=2,label=’SFM’)
plt.axis([0,n*timeStep,min(friction_d_sfm)-0.1,max(friction_d_sfm)+0.1])
plt.legend(loc=4,fontsize=14)
plt.xticks(fontsize=12)
plt.yticks(fontsize=12)
plt.ylabel(’f$_d$’,fontsize=14)

plt.subplot(413)
plt.plot(time[H+1:n],choke_pressure_input[H+1:n],’k-’,lw=2)
plt.axis([0,n*timeStep,np.floor(np.min(choke_pressure_input))-5,
      np.ceil(np.max(choke_pressure_input))+5])
plt.xticks(fontsize=12)
plt.yticks(fontsize=12)
plt.ylabel(’P$_{choke}$ (bar)’,fontsize=14)

plt.subplot(414)
plt.plot(time[H+1:n],mud_flow_in[H+1:n],’k-’,lw=2)
plt.axis([0,n*timeStep,np.floor(np.min(mud_flow_in))-10,
       np.ceil(np.max(mud_flow_in))+10])
plt.xticks(fontsize=12)
plt.yticks(fontsize=12)
```

المنارة للاستشارات
www.manaraa.com

```
plt.xlabel('Time (s)',fontsize=14)
plt.ylabel('q$_p$ (l/m)',fontsize=14)

plt.savefig('MPC2.png', format='png', dpi=400, bbox_inches='tight')
plt.savefig('MPC2.eps', format='eps', dpi=400, bbox_inches='tight')

well_model.hfm_shutdown()
sfm_mhe.sfm_shutdown()
sfm_mpc.sfm_shutdown()
```

## B.2 SFM MHE Code

```
### IMPORTS ###
import numpy as np
import ctypes
import os
from _ctypes import FreeLibrary
from scipy.optimize import minimize

dllfile = 'SM_Wrapper64r.dll'
configurationfile='CaseG.wel'
cd = os.getcwd()
model_Path = os.path.realpath('SFM_mhe')
dll = ctypes.WinDLL(os.path.join(model_Path, dllfile))
pSimplifiedModel = dll.simplifiedWrapper_Create(ctypes.c_char_p(model_Path))
dll.setDouble(pSimplifiedModel,
    ctypes.c_char_p("BoundaryCondition"),ctypes.c_double(7))

h = open(os.path.join(model_Path + '\InputFileName.in'),'w')
h.write(configurationfile)
h.close()
```

www.manaraa.com

```
class sfm_meas():
    t = 0
    q_p = 0
    q_choke = 0
    spp = 0
    bh_ECD = 0
    p_c = 0
    p_bit = 0
    pSimplifiedModel = pSimplifiedModel
    dll = dll

### initialize flow model
def mhe_run(well_input,mhe_input,e_ig,H):
    ### Run Well
    x = np.zeros(43)
    x = x + -999

    x[1] = well_input.time - well_input.TimeStep*H
    x[2] = well_input.bitposition - (well_input.TimeStep*24.)*well_input.ROP*H
    x[5] = well_input.rotary_speed *2.*np.pi/60.  # [rad/s]
    x[8] = well_input.mudflowin / (1000. * 60.)   # [m3/s]
    x[9] = well_input.mud_density_in *1000.       # [kg/m3]
    x[10] = well_input.depthhole                  # [m]
    x[11] = well_input.desired_emw * 1000.        # [kg/m3]
    x[17] = well_input.choke_press * 1e5          # [Pa]
    x[20] = well_input.input_mud_temp +273.15     # [K]
    x[23] = well_input.cross_flow / (1000. * 60.)   # [m3/s]
    x[30] = well_input.set_point_position

    if mhe_input.FV1_sw == 1 and mhe_input.FV2_sw == 0:
        dll.setDouble(pSimplifiedModel,ctypes.c_char_p("CalibratedFrictionFactorAnnulus"),
```

www.manaraa.com

```
    ctypes.c_double(e_ig[0]))
    dll.setDouble(pSimplifiedModel,types.c_char_p("CalibratedFrictionFactorDrillString"),
    ctypes.c_double(mhe_input.friction_d))
if mhe_input.FV1_sw == 0 and mhe_input.FV2_sw == 1:
    dll.setDouble(pSimplifiedModel,
        ctypes.c_char_p("CalibratedFrictionFactorAnnulus"),
    ctypes.c_double(mhe_input.friction_a))
    dll.setDouble(pSimplifiedModel,
        ctypes.c_char_p("CalibratedFrictionFactorDrillString"),
    ctypes.c_double(e_ig[1]))
if mhe_input.FV1_sw ==1 and mhe_input.FV2_sw == 1:
    dll.setDouble(pSimplifiedModel,
        ctypes.c_char_p("CalibratedFrictionFactorAnnulus"),
    ctypes.c_double(e_ig[0]))
    dll.setDouble(pSimplifiedModel,
        ctypes.c_char_p("CalibratedFrictionFactorDrillString"),
    ctypes.c_double(e_ig[1]))

realTable_well = (ctypes.c_double * len(x))(*x)
dll.run(pSimplifiedModel, ctypes.byref(realTable_well))
C_Out_SFM =  (ctypes.c_double * 8)(*np.zeros(8))
dll.getRealTimeParameters(pSimplifiedModel,ctypes.byref(C_Out_SFM))

###Prep data for output
sfm_meas.t     = C_Out_SFM[0]   # [min]
sfm_meas.q_p     = C_Out_SFM[1]   # [lpm]
sfm_meas.q_choke = C_Out_SFM[2]  # [lpm]
sfm_meas.spp     = C_Out_SFM[3]   # [bar]
sfm_meas.bh_ECD = C_Out_SFM[4]  # [kg/m3]
sfm_meas.p_c     = C_Out_SFM[5]   # [bar]
sfm_meas.p_bit = C_Out_SFM[6]   # [bar]
```

المنارة للاستشارات
www.manaraa.com

```
    return sfm_meas

## Controller Function ###
def estimate(e_ig, well_input, mhe_input, measured, ctlr_moves, H, k):
    bnds = [(0.05,10.0),(0.05,10.0)]
    est = minimize(predictions, e_ig, args=(well_input, mhe_input, measured,
        ctlr_moves, H, k), method='SLSQP',bounds=bnds,options={'disp': False,
        'eps':1.0e-09,'maxiter': 100, 'ftol':.05})
    ff = est.x
    return ff

def predictions(e_ig, well_input, mhe_input, measured, ctlr_moves, H, k):
    dll.loadState(pSimplifiedModel)

    predictions.spp    = np.zeros(H)   # [bar]
    predictions.q_p    = np.zeros(H)   # [lpm]
    predictions.p_c    = np.zeros(H)   # [bar]
    predictions.q_choke = np.zeros(H)
    predictions.p_bit = np.zeros(H)
    se = np.zeros(H)

    ### Run Well
    for j in range(0,H):
        mhe_input.time = well_input.time + well_input.TimeStep*(j-H)
        mhe_input.bitposition = well_input.bitposition -
            (well_input.TimeStep*24.)*well_input.ROP*H +
            (well_input.TimeStep*24.)*well_input.ROP
        mhe_input.depthhole = mhe_input.bitposition

        x = np.zeros(43)
        x = x + -999
```

المنارة للاستشارات
www.manaraa.com

```
x[1] = mhe_input.time
x[2] = mhe_input.bitposition
x[5] = mhe_input.rotary_speed *2.*np.pi/60. # [rad/s]
x[8] = ctlr_moves[1,(-H+j)]/(1000*60)    # [m3/s]
x[9] = mhe_input.mud_density_in *1000.     # [kg/m3]
x[10] = mhe_input.depthhole              # [m]
x[11] = mhe_input.desired_emw * 1000.    # [kg/m3]
x[17] = ctlr_moves[0,(-H+j)] * 1.0e5     # [Pa]
x[20] = mhe_input.input_mud_temp +273.15  #[K]
x[23] = mhe_input.cross_flow / (1000. * 60.) # [m3/s]
x[30] = mhe_input.set_point_position

if mhe_input.FV1_sw == 1 and mhe_input.FV2_sw == 0:
    dll.setDouble(pSimplifiedModel,
        ctypes.c_char_p("CalibratedFrictionFactorAnnulus"),
        ctypes.c_double(e_ig[0]))
    dll.setDouble(pSimplifiedModel,
        ctypes.c_char_p("CalibratedFrictionFactorDrillString"),
        ctypes.c_double(mhe_input.friction_d))
if mhe_input.FV1_sw == 0 and mhe_input.FV2_sw == 1:
    dll.setDouble(pSimplifiedModel,
        ctypes.c_char_p("CalibratedFrictionFactorAnnulus"),
        ctypes.c_double(mhe_input.friction_a))
    dll.setDouble(pSimplifiedModel,
        ctypes.c_char_p("CalibratedFrictionFactorDrillString"),
        ctypes.c_double(e_ig[1]))
if mhe_input.FV1_sw ==1 and mhe_input.FV2_sw == 1:
    dll.setDouble(pSimplifiedModel,
        ctypes.c_char_p("CalibratedFrictionFactorAnnulus"),
        ctypes.c_double(e_ig[0]))
```

المنارة للاستشارات
www.manaraa.com

```
    dll.setDouble(pSimplifiedModel,
        ctypes.c_char_p("CalibratedFrictionFactorDrillString"),
        ctypes.c_double(e_ig[1]))

realTable_well = (ctypes.c_double * len(x))(*x)
dll.run(pSimplifiedModel, ctypes.byref(realTable_well))
P_Out_SFM =  (ctypes.c_double * 8)(*np.zeros(8))
dll.getRealTimeParameters(pSimplifiedModel,ctypes.byref(P_Out_SFM))

predictions.q_p[j]   = P_Out_SFM[1]
predictions.q_choke[j] = P_Out_SFM[2] # [lpm]
predictions.spp[j]   = P_Out_SFM[3]  # [bar]
predictions.p_c[j]   = P_Out_SFM[5]
predictions.p_bit[j] = P_Out_SFM[6]

if mhe_input.SV1_sw == 1 and mhe_input.SV2_sw == 0:
    if mhe_input.FV1_sw == 1 and mhe_input.FV2_sw == 0:
        se[j] = (measured[0,(j)] - predictions.p_bit[(j)])**2 +
            100*(measured[2,H-1]-e_ig[0])**2
    if mhe_input.FV1_sw == 0 and mhe_input.FV2_sw == 1:
        se[j] = (measured[0,(j)] - predictions.p_bit[(j)])**2 +
            100*(measured[3,H-1]-e_ig[1])**2
if mhe_input.SV1_sw == 0 and mhe_input.SV2_sw == 1:
    if mhe_input.FV1_sw == 1 and mhe_input.FV2_sw == 0:
        se[j] = (measured[1,(j)] - predictions.spp[(j)])**2 +
            200*(measured[2,H-1]-e_ig[0])**2
    if mhe_input.FV1_sw == 0 and mhe_input.FV2_sw == 1:
        se[j] = (measured[1,(j)] - predictions.spp[(j)])**2 +
            1000*(measured[3,H-1]-e_ig[1])**2
    if mhe_input.FV1_sw == 1 and mhe_input.FV2_sw == 1:
```

www.manaraa.com

```
                se[j] = (measured[1,(j)] - predictions.spp[(j)])**2 +
                    500*(measured[2,H-1]-e_ig[0])**2 +
                    200*(measured[3,H-1]-e_ig[1])**2
        if mhe_input.SV1_sw == 1 and mhe_input.SV2_sw == 1:
            if mhe_input.FV1_sw == 1 and mhe_input.FV2_sw == 1:
                se[j] = 2000*(measured[0,(j)] - predictions.p_bit[(j)])**2 + 1000*
                    (measured[1,(j)] - predictions.spp[(j)])**2 +
                    2000*(measured[2,H-1]-e_ig[0])**2 +
                    500*(measured[3,H-1]-e_ig[1])**2

    obj = np.sum(se)

    return obj

def sfm_save():
    dll.saveState(pSimplifiedModel)

def sfm_load():
    dll.loadState(pSimplifiedModel)

def sfm_shutdown():
    dll.simplifiedWrapper_Destroy(pSimplifiedModel)
    FreeLibrary(dll._handle)
    return
```

## B.3 SFM MPC Code

```
### IMPORTS ###
import numpy as np
import ctypes
import os
```

المنارة للاستشارات

www.manaraa.com

```
from _ctypes import FreeLibrary
from scipy.optimize import minimize

dllfile = ’SM_Wrapper64r.dll’
configurationfile=’CaseG.wel’
cd = os.getcwd()
model_Path = os.path.realpath(’SFM_mpc’)
dll = ctypes.WinDLL(os.path.join(model_Path, dllfile))
pSimplifiedModel = dll.simplifiedWrapper_Create(ctypes.c_char_p(model_Path))
dll.setDouble(pSimplifiedModel,
    ctypes.c_char_p("BoundaryCondition"),ctypes.c_double(7))

h = open(os.path.join(model_Path + ’\InputFileName.in’),’w’)
h.write(configurationfile)
h.close()

class sfm_meas():

    t = 0
    q_p = 0
    q_choke = 0
    spp = 0
    bh_ECD = 0
    p_c = 0
    p_bit = 0
    pSimplifiedModel = pSimplifiedModel
    dll = dll

### initialize flow model
def mpc_run(mpc_input):
    ### Run Well
    x = np.zeros(43)
```

www.manaraa.com

```
x = x + -999

x[1] = mpc_input.time
x[2] = mpc_input.bitposition
x[5] = mpc_input.rotary_speed *2.*np.pi/60. # [rad/s]
x[8] = mpc_input.mudflowin / (1000. * 60.) # [m3/s]
x[9] = mpc_input.mud_density_in *1000.   # [kg/m3]
x[10] = mpc_input.depthhole              # [m]
x[11] = mpc_input.desired_emw * 1000.    # [kg/m3]
x[17] = mpc_input.choke_press * 1e5    # [Pa]
x[20] = mpc_input.input_mud_temp +273.15  # [K]
x[23] = mpc_input.cross_flow / (1000. * 60.) # [m3/s]
x[30] = mpc_input.set_point_position

dll.setDouble(pSimplifiedModel,
    ctypes.c_char_p("CalibratedFrictionFactorAnnulus"),
    ctypes.c_double(mpc_input.friction_a))
dll.setDouble(pSimplifiedModel,
    ctypes.c_char_p("CalibratedFrictionFactorDrillString"),
    ctypes.c_double(mpc_input.friction_d))


realTable_well = (ctypes.c_double * len(x))(*x)
dll.run(pSimplifiedModel, ctypes.byref(realTable_well))
C_Out_SFM =  (ctypes.c_double * 8)(*np.zeros(8))
dll.getRealTimeParameters(pSimplifiedModel,ctypes.byref(C_Out_SFM))

###Prep data for output
sfm_meas.t     = C_Out_SFM[0]  # [min]
sfm_meas.q_p   = C_Out_SFM[1]  # [lpm]
sfm_meas.q_choke = C_Out_SFM[2] # [lpm]
sfm_meas.spp   = C_Out_SFM[3]  # [bar]
```

المنارة للاستشارات
www.manaraa.com

```
    sfm_meas.bh_ECD = C_Out_SFM[4]  # [kg/m3]
    sfm_meas.p_c   = C_Out_SFM[5]   # [bar]
    sfm_meas.p_bit = C_Out_SFM[6]   # [bar]

    return sfm_meas

## Controller Function ###
def control(x_ig,well_input,mpc_input, P, k):

    if mpc_input.mpc_sw == 1:
        choke_lower = np.ones(P)*0.0
        choke_upper = np.ones(P)*300.0

        mud_lower = np.ones(P)*0.0
        mud_upper = np.ones(P)*3000.0

        lower_bnds = np.append(choke_lower,mud_lower)
        upper_bnds = np.append(choke_upper,mud_upper)

        bnds = zip(lower_bnds,upper_bnds)

        control = minimize(predictions, x_ig, args=(mpc_input, well_input, P, k),
            method='SLSQP', jac=None, bounds=bnds, tol=0.01, options={'disp':
            False, 'eps':1.0e-09,'maxiter': 100, 'ftol':.05})

        p_c_hat = control.x[0:P]
        q_p_hat = control.x[P:]

    else:
        q_p_hat = x_ig[1,:]
        p_c_hat = x_ig[0,:]
```

المنارة للاستشارات
www.manaraa.com

```
    x_ig = np.row_stack((p_c_hat,q_p_hat))

    return x_ig


def predictions(x_ig, mpc_input, well_input, P, k):

    dll.loadState(pSimplifiedModel)

    p_bit_hat = np.zeros(P)
    SP_hat = np.zeros(P) + mpc_input.SP
    se = np.zeros(P)

    ### Run Well
    for j in range(0,P):
        mpc_input.time = well_input.time + (mpc_input.TimeStep *(j))

        mpc_input.bitposition = well_input.bitposition +
            (mpc_input.TimeStep*24.)*mpc_input.ROP
        mpc_input.depthhole = mpc_input.bitposition

        x = np.zeros(43)
        x = x + -999

        x[1] = mpc_input.time
        x[2] = mpc_input.bitposition
        x[5] = mpc_input.rotary_speed *2.*np.pi/60. # [rad/s]
        x[8] = x_ig[j+P]/(1000*60)             # [m3/s]
        x[9] = mpc_input.mud_density_in *1000.     # [kg/m3]
        x[10] = mpc_input.depthhole               # [m]
        x[11] = mpc_input.desired_emw * 1000.     # [kg/m3]
        x[17] = x_ig[j] * 1.0e5             # [Pa]
```

المنارة للاستشارات
www.manaraa.com

```
        x[20] = mpc_input.input_mud_temp +273.15   # [K]
        x[23] = mpc_input.cross_flow / (1000. * 60.)  # [m3/s]
        x[30] = mpc_input.set_point_position
        dll.setDouble(pSimplifiedModel,
            ctypes.c_char_p("CalibratedFrictionFactorAnnulus"),
            ctypes.c_double(mpc_input.friction_a))
        dll.setDouble(pSimplifiedModel,
            ctypes.c_char_p("CalibratedFrictionFactorDrillString"),
            ctypes.c_double(mpc_input.friction_d))


        realTable_well = (ctypes.c_double * len(x))(*x)
        dll.run(pSimplifiedModel, ctypes.byref(realTable_well))
        P_Out_SFM =  (ctypes.c_double * 8)(*np.zeros(8))
        dll.getRealTimeParameters(pSimplifiedModel,ctypes.byref(P_Out_SFM))

        p_bit_hat[j]  = P_Out_SFM[6]  # [bar]

        # Squared Error
        if j > 0:
            se[j]  = 1000*(SP_hat[j]-p_bit_hat[j])**2 + 100*(x_ig[j]-x_ig[j-1])**2
                + 0.1*(x_ig[j+P]-x_ig[j+P-1])**2

        else:
            se[j]  = 1000*(SP_hat[j]-p_bit_hat[j])**2 +
                100*(x_ig[j]-well_input.choke_press)**2 +
                0.1*(x_ig[j+P]-well_input.mudflowin)**2

    obj = np.sum(se)
    return obj

def sfm_save():
```

المنارة للاستشارات
www.manaraa.com

```
    dll.saveState(pSimplifiedModel)


def sfm_load():
    dll.loadState(pSimplifiedModel)


def sfm_shutdown():
    dll.simplifiedWrapper_Destroy(pSimplifiedModel)
    FreeLibrary(dll._handle)
    return
```

## B.4 HFM Well Simulation Code

```
### IMPORTS ###
import ctypes
import os
import numpy as np
from _ctypes import FreeLibrary


dllfile = ’FlowModel64r.dll’
configurationfile = ’CaseG.wel’
model_instance = ’HFM’


class well_meas():
    flowout_well = 0
    pres_well = 0
    gas_influx = 0
    p_bit = 0
    p_c = 0
    h_bit = 0
    q_choke = 0
    pit_gain = 0
```

المنارة للاستشارات
www.manaraa.com

```
    surge_vol = 0
    mudflowin = 0
    friction_factor = 0
    p_choke = 0
    pit_gain = 0
    spp = 0
    dll = 0

### creating quasi header file
class DataStructureOut(ctypes.Structure):
    _fields_ = [(’bhEcdCalc’,ctypes.c_double),
               (’bhTempCalc’,ctypes.c_double),
               (’csEcdCalc’,ctypes.c_double),
               (’csTempCalc’,ctypes.c_double),
               (’pitGainCalc’,ctypes.c_double),
               (’sppCalc’,ctypes.c_double),
               (’flowOutCalc’,ctypes.c_double),
               (’tempOutCalc’,ctypes.c_double),
               (’cmpLiftHeight’,ctypes.c_double),
               (’cmpPresSet’,ctypes.c_double),
               (’cmpSucPCalc’,ctypes.c_double),
               (’cmpRpmCalc’,ctypes.c_double),
               (’cmpPowCalc’,ctypes.c_double),
               (’cmpSurgeVolCalc’,ctypes.c_double),
               (’pChoke’,ctypes.c_double),
               (’frictionFactor’,ctypes.c_double),
               (’bhPresCalc’,ctypes.c_double),
               (’csPresCalc’,ctypes.c_double),
               (’ropCalc’,ctypes.c_double),
               (’diffWellPoreEmwCalc’,ctypes.c_double),
               (’diffFracWellEmwCalc’,ctypes.c_double),
               (’surgeVolCalc’,ctypes.c_double),
```

المنارة للاستشارات
www.manaraa.com

```
               (’tvdBottomCalc’,ctypes.c_double),
               (’pwdPresCalc’,ctypes.c_double),
               (’pwdTempCalc’,ctypes.c_double),
               (’volBlanketRiserCalc’,ctypes.c_double),
               (’levelMudRiserCalc’,ctypes.c_double),
               (’volMudRiserCalc’,ctypes.c_double),
               (’volCMPRetLineCalc’,ctypes.c_double),
               (’ecdAtPosCalc’,ctypes.c_double),]

###Find or create the file path to the case file
cd = os.getcwd()
model_Path = os.path.realpath(’HFM’)
test = os.path.exists(os.path.join(cd,model_instance))
if test == False:
    os.makedirs(os.path.join(cd,model_instance))

h = open(os.path.join(cd,model_instance + ’\InputFileName.in’),’w’)
h.write(configurationfile)
h.close()
print model_Path

### Load dll
dll = ctypes.WinDLL(os.path.join(model_Path,dllfile))
### initialize flow model
dll.setmodulestring(ctypes.c_char_p(’FilePath’),ctypes.c_int(8),
                  ctypes.c_char_p(model_Path),
                  ctypes.c_int(len(model_Path)),
                  ctypes.c_int(0))

realtimeDataStructureOut = DataStructureOut(ctypes.c_double(-999.99),
                                        ctypes.c_double(-999.99),
                                        ctypes.c_double(-999.99),
```

المنارة للاستشارات

www.manaraa.com

```
                                        ctypes.c_double(-999.99),
                                        ctypes.c_double(-999.99),
                                        ctypes.c_double(-999.99),
                                        ctypes.c_double(-999.99),
                                        ctypes.c_double(-999.99),
                                        ctypes.c_double(-999.99),
                                        ctypes.c_double(-999.99),
                                        ctypes.c_double(-999.99),
                                        ctypes.c_double(-999.99),
                                        ctypes.c_double(-999.99),
                                        ctypes.c_double(-999.99),
                                        ctypes.c_double(-999.99),
                                        ctypes.c_double(-999.99),
                                        ctypes.c_double(-999.99),
                                        ctypes.c_double(-999.99),
                                        ctypes.c_double(-999.99),
                                        ctypes.c_double(-999.99),
                                        ctypes.c_double(-999.99),
                                        ctypes.c_double(-999.99),
                                        ctypes.c_double(-999.99),
                                        ctypes.c_double(-999.99),
                                        ctypes.c_double(-999.99),
                                        ctypes.c_double(-999.99),
                                        ctypes.c_double(-999.99),
                                        ctypes.c_double(-999.99),
                                        ctypes.c_double(-999.99),
                                        ctypes.c_double(-999.99))
dll.setmoduletable(ctypes.c_char_p('Use_measured_choke_pressure_as_boundary'),
                 ctypes.c_int(39),
                 ctypes.byref(ctypes.c_double(1)),
                 ctypes.c_int(1),
                 ctypes.c_int(0),
```

المنارة للاستشارات

www.manaraa.com

```
                ctypes.c_bool(0))

### initialize flow model
def well_run(well_input):
    ### Run Well
    x = np.zeros(44)
    x = x + -999
    x[0] = 0
    x[1] = well_input.time
    x[2] = well_input.bitposition
    x[5] = well_input.rotary_speed*2.*np.pi/60. # [rad/s]
    x[8] = well_input.mudflowin / (1000. * 60.) # [m3/s]
    x[9] = well_input.mud_density_in*1000.  # [kg/m3]
    x[10] = well_input.depthhole      # [m]
    x[11] = well_input.desired_emw * 1000.   # [kg/m3]
    x[17] = well_input.choke_press * 1e5   # [Pa]
    x[20] = well_input.input_mud_temp +273.15 # [K]
    x[30] = well_input.set_point_position   # [m]
    x[43] = 0

    realTable_well = (ctypes.c_double * len(x))(*x)
    friction = well_input.friction_a

    tempmode = 0
    XX = np.array([-999, -999, -999, tempmode, -999, -999, -999, friction])
    config = (ctypes.c_double * len(XX))(*XX)
    dll.setmoduletable(ctypes.c_char_p(’Input_Configur’), ctypes.c_int(14),
        ctypes.byref(config), ctypes.c_int(0), ctypes.c_int(7), ctypes.c_bool(0))

    TimeP_well = ctypes.c_double(0)
    ### Input values into flow model
```

www.manaraa.com

```
dll.setmoduletable(ctypes.c_char_p('Input_RealTime'), ctypes.c_int(14),
    ctypes.byref(realTable_well), ctypes.c_int(43), ctypes.c_int(0),
    ctypes.c_bool(0))
### Execute flow model
dll.runflowmodel(ctypes.byref(TimeP_well),ctypes.c_int(2),ctypes.byref(ctypes.c_double(0)),
### Get data from flow model
#print(TimeP_well.value)
dll.getrealtimeparameters(ctypes.byref(realtimeDataStructureOut),ctypes.c_int(6))
### realtimeDataStructureOut is now updated with all values

### Read choke pressure
obs_points = np.array([0])
observationPoints = (ctypes.c_int * len(obs_points))(*obs_points)
sensordata = ctypes.c_double(-999.99)
statusP = ctypes.byref(ctypes.c_int(0))
for d in range(len(observationPoints)):
    dll.getmodulearray(ctypes.c_char_p('DataAtPos_pres'),
        ctypes.byref(ctypes.c_int(14)), ctypes.byref(observationPoints),
        ctypes.byref(sensordata), statusP)

###Prep data for output
well_meas.h_bit = well_input.bitposition
well_meas.p_bit = realtimeDataStructureOut.bhPresCalc/100000
well_meas.p_c = sensordata.value/100000
well_meas.friction_factor = realtimeDataStructureOut.frictionFactor
well_meas.dll = dll
well_meas.spp = realtimeDataStructureOut.sppCalc
well_meas.flowout_well = realtimeDataStructureOut.flowOutCalc
well_meas.p_choke = realtimeDataStructureOut.pChoke
well_meas.pit_gain = realtimeDataStructureOut.pitGainCalc

return well_meas
```

www.manaraa.com

```
def hfm_save():
    dll.setmoduletable(ctypes.c_char_p('Save_stateMemory'), ctypes.c_int(15),
        ctypes.byref(ctypes.c_double(1)), ctypes.c_int(0), ctypes.c_int(0),
        ctypes.c_bool(0))

def hfm_load():
    dll.setmoduletable(ctypes.c_char_p('Load_stateMemory'), ctypes.c_int(15),
        ctypes.byref(ctypes.c_double(1)), ctypes.c_int(0), ctypes.c_int(0),
        ctypes.c_bool(0))

def hfm_shutdown():
    dll.enddll()
    FreeLibrary(dll._handle)
    return
```

المنارة للاستشارات
www.manaraa.com